The Astrophysical Journal, 464:641–663, 1996 June 20

GASDYNAMICS AND STARBURSTS IN MAJOR MERGERS

J. Christopher Mihos[1,2] and Lars Hernquist[3]
Board of Studies in Astronomy and Astrophysics, University of California, Santa Cruz, CA 95064;
hos@pha.jhu.edu, lars@lick.ucsc.edu
Received 1995 July 10; accepted 1996 January 16

ABSTRACT

Using numerical simulation, we study the development of gaseous inflows and triggering of starburst activity in mergers of disk galaxies of comparable mass. Our models cover a range of orbits and internal structures for the merging galaxies. In all encounters studied, the galaxies experience strong gaseous inflows and, using a density-dependent Schmidt law to model star formation, moderate to intense starburst activity. We find that galaxy structure plays a dominant role in regulating activity. The gaseous inflows are strongest when galaxies with dense central bulges are in the final stages of merging, while inflows in bulgeless galaxies are weaker and occur earlier in the interaction. Orbital geometry plays only a relatively modest role in the onset of collisionally induced activity. Through an analysis of the torques acting on the gas, we show that these inflows are generally driven by gravitational torques from the host galaxy (rather than the companion) and that dense bulges act to stabilize galaxies against bar modes and inflow until the galaxies merge, at which point rapidly varying gravitational torques drive strong dissipation and inflow of gas in the merging pair. The strongest inflows (and associated starburst activity) develop in coplanar encounters, while the activity in inclined mergers is somewhat less intense and occurs slightly later during the merger. To the extent that a Schmidt law is a reasonable description of star formation in these systems, the starbursts that develop in mergers of galaxies with central bulges represent an increase in the star formation rate of two orders of magnitude over that in isolated galaxies. We find that the gaseous and stellar morphology and star-forming properties of these systems provide a good match to those of observed ultraluminous infrared galaxies. Our results imply that the internal structure of the merging galaxies, rather than orbital geometry, may be the key factor in producing ultraluminous infrared galaxies.

Subject headings: galaxies: active — galaxies: interactions — galaxies: starburst — galaxies: structure — methods: numerical

1. INTRODUCTION

Collisions and mergers of galaxies are thought to play a crucial role in the onset of certain unusual phenomena in galaxies, specifically starbursts and the occurrence of nuclear activity. The optical and infrared colors of many peculiar galaxies can be understood in terms of bursts of star formation triggered by galaxy encounters (Larson & Tinsley 1978; Joseph et al. 1984). Colliding galaxies often display higher levels of Hα emission (see, e.g., Kennicutt et al. 1987; Bushouse 1987), radio continuum emission (Hummel 1981; Condon et al. 1982), and infrared emission (Lonsdale, Persson, & Matthews 1984; Solomon & Sage 1988) than isolated galaxies, indicative of strong star formation activity (see, e.g., Joseph & Wright 1985; Joseph 1990). Many of the far-infrared luminous galaxies identified by *IRAS* are found to be undergoing collisions (see, e.g., Soifer et al. 1984a, b; Sanders et al. 1986, 1988a, b; Armus, Heckman, & Miley 1987; Kleinmann et al. 1988). Furthermore, the fraction of interacting systems found in *IRAS*-selected samples increases with luminosity (Lawrence et al. 1989), which suggests that collisions play a major role in triggering powerful starbursts. In fact, the brightest infrared-luminous objects, with quasar-like infrared luminosities of $L_{\rm FIR} > 10^{12}\ L_{\odot}$, all show morphological peculiarities indicative of encounters, such as multiple nuclei and tidal features (Sanders et al. 1988b; Melnick & Mirabel 1990). Millimeter CO observations of these galaxies have revealed massive pools of molecular gas in their central regions (see, e.g., Sanders et al. 1987; Sargent & Scoville 1991; Scoville et al. 1991), providing fuel for starbursts or ultimately perhaps AGN activity. However, not all interacting systems show elevated tracers of star formation (Keel et al. 1985; Bushouse 1986; Kennicutt et al. 1987), which raises questions about the detailed nature of the starburst triggering mechanism.

Evidence also exists linking collisions and mergers to the onset of nuclear activity in galaxies (see Stockton 1990; Barnes & Hernquist 1992a; Osterbrock 1993 for reviews). A variety of studies suggest that Seyfert galaxies are preferentially found in interacting systems (see, e.g., Dahari 1984; Kennicutt & Keel 1984; MacKenty 1989). Investigations of the environments of quasar host galaxies also reveal an excess of companion galaxies (McLeod & Rieke 1994; Hutchings, Crampton, & Johnson 1995; Bahcall, Kirhakos, & Schneider 1995a), and many Seyferts, quasars, and radio galaxies exhibit signs of encounters and mergers in the form of tidal debris and multiple nuclei (van Albada, Kotanyi, & Schwarzschild 1982; Smith & Heckman 1989a, b; MacKenty 1990; Hutchings & Neff 1992; Armus et al. 1994; Bahcall, Kirhakos, & Schneider 1995b). In fact, the most luminous IR galaxies may actually harbor buried AGNs (see, e.g., Sanders et al. 1988b; Leech et al. 1989; Veilleux et al. 1995), which suggests a possible evolutionary link between mergers, luminous IR galaxies, and quasars (see, e.g., Sanders, Soifer, & Neugebauer 1990).

It is clear from the observations that gasdynamics and star formation in mergers must be responsible for much of

[1] Hubble Fellow.
[2] Current address: Department of Physics and Astronomy, Johns Hopkins University, Baltimore, MD 21218.
[3] Alfred P. Sloan Foundation Fellow; Presidential Faculty Fellow.

the behavior associated with active galaxies. In addition, these processes may also be quite important for interpreting many aspects of ordinary galaxies. As one example, the "merger hypothesis" for the origin of early-type galaxies argues that present-day ellipticals form primarily from mergers of disk galaxies (Toomre 1977; Schweizer 1982, 1990). The tendency for mergers to produce remnants possessing $r^{1/4}$ surface brightness profiles has been well demonstrated both observationally (see, e.g., Wright et al. 1990; Stanford & Bushouse 1991) and theoretically (see, e.g., Barnes 1988, 1992; Hernquist 1992, 1993a). Furthermore, many ellipticals exhibit low surface brightness loops and shells (Malin & Carter 1980; Schweizer & Seitzer 1988) that are thought to form naturally during disk galaxy mergers (Hernquist & Spergel 1992; Hibbard & Mihos 1995). However, the merger hypothesis in its simplest form suffers from a serious defect: the central phase space density in stellar disk galaxies is much lower than the observed central phase space density of ellipticals, so mergers of pure stellar disks produce remnants less centrally concentrated in phase space than real ellipticals (Carlberg 1986; Gunn 1987; Hernquist, Spergel, & Heyl 1993). In principle, this objection can be overcome if gaseous dissipation and a starburst during a merger act to increase the central stellar density of the remnant (Kormendy & Sanders 1992).

The role played by merger-driven gasdynamics and starbursts in shaping normal galaxies may be manifested in other ways as well. The kinematically distinct cores observed in many elliptical galaxies (see, e.g., Kormendy 1984; Franx & Illingworth 1988; Bender 1990a, b; Forbes, Franx, & Illingworth 1995) may be formed through dissipation and subsequent central starbursts (Hernquist & Barnes 1991; Mihos & Hernquist 1994c). Such processes may also give rise to gradients in color profiles (Franx, Illingworth, & Heckman 1989; Peletier et al. 1990), metallicity profiles (Bender & Surma 1992; Davies et al. 1993; Mihos & Hernquist 1994d; Surma & Bender 1995), and the mean age of the stellar populations in galaxies. Farther from the galaxy center, induced star formation may lead to the formation of young globular clusters (see, e.g., Ashman & Zepf 1992; Whitmore et al. 1993) and perhaps even dwarf irregular galaxies in tidal tails (Zwicky 1956; Schweizer 1978; Mirabel, Dottori, & Lutz 1992; Barnes & Hernquist 1992b; Elmegreen, Kaufman, & Thomasson 1993). Minor mergers may also "sweep" galactic disks clean of cold gas, transforming late-type disk galaxies into earlier Sa or S0 galaxies (Hernquist 1989; Mihos & Hernquist 1994a). Therefore, any attempt to model the relationship between galaxy collisions and violent activity or galaxy evolution must ultimately account for the effects of dissipation and star formation.

Theoretical work on these problems is relatively new. Early attempts to include gasdynamics in mergers utilized a "sticky particle" approach for the evolution of the gas (see, e.g., Negroponte & White 1983; Noguchi 1988). More sophisticated techniques employed smoothed particle hydrodynamics (SPH) to follow the evolution of the ISM in merging galaxies (Barnes & Hernquist 1991, 1995), giving a more complete description of the physical conditions in the gaseous components of the galaxies. These studies reinforce the notion that galaxy mergers can drive significant inflows of gas under a wide range of conditions. The first calculations to include star formation and gas depletion in merging galaxies (see, e.g., Noguchi & Ishibashi 1986; Noguchi 1991; Olson & Kwan 1990a, b; Mihos, Richstone, & Bothun 1992; Mihos, Bothun, & Richstone 1993; Mihos 1992) indicated that star formation rates can be raised by more than an order of magnitude during a merger and that these starbursts can significantly deplete the galaxies of cold gas. However, these later star-forming simulations all employed sticky particle hydrodynamics and relatively crude galaxy models, and, moreover, suffered from limited kinematic and spatial resolution because of the relatively small number of particles used in the simulations (typically $N \sim 1\text{–}3 \times 10^4$).

Here we expand on previous studies to assess more generally the nature of merger-induced gas inflows and starbursts and to make predictions that may be tested observationally. We employ a more physical description of the relevant physics and employ galaxy models that are more realistic than those that have been used previously. In particular, we incorporate a prescription for star formation into the hydrodynamical model for the ISM that allows us to follow the full evolution of the merging galaxies, including the production of a young starburst population. Furthermore, we use fully self-consistent galaxy models, with structural properties chosen to mimic the observed properties of nearby disk galaxies. These improvements enable us to investigate the detailed dynamics responsible for driving inflow and starburst activity during galaxy mergers.

In this paper we focus on "major mergers"—mergers involving galaxies of comparable mass—in view of their likely relevance to ultraluminous infrared galaxies and the formation of elliptical galaxies. We survey mergers of pairs of disk galaxies having dark matter halos and, optionally, dense compact bulges. In each case considered, we find that the interaction and subsequent merger initiates a strong inflow of gas into the nucleus of the remnant, triggering intense but short-lived bursts of star formation. We isolate the physics responsible for these inflows and demonstrate that their history depends sensitively on the structure of the progenitor galaxies. We also investigate the effects of orbital geometry by varying the inclination of the merging disks and find that starbursts occur generically in encounters that lead to rapid merging.

We compare our results to those of previous theoretical work and consider their relation to observations of starbursting and active galaxies. In particular, we show that the emission from the ultraluminous infrared galaxies can be plausibly explained by merger-induced starbursts, without invoking a nonthermal energy source (i.e., an AGN). Although our models cannot follow the evolution of the nuclear gas on parsec scales, if dissipation continues to act on the gas in those regions, our results may also be applicable to the triggering and fueling of active nuclei in galaxies. Finally, we examine how our results depend on the assumptions and limitations inherent to our models, and summarize questions for future interest.

2. NUMERICAL TECHNIQUE

Modeling the full evolution of galaxy mergers involves many distinct physical processes, including gravitational dynamics, the hydrodynamics of the ISM, and star formation. To follow these coupled effects, the simulations described in this paper were performed using a hybrid N-body/hydrodynamics code known as TREESPH (Hernquist & Katz 1989), modified to include star formation in the gas (Mihos & Hernquist 1994e). We include here a brief description of the numerical techniques; for a more thorough discussion, we refer the reader to the above references.

2.1. *TREESPH*

To model composite systems of gas, stars, and dark matter, TREESPH uses a hierarchical tree method (Barnes & Hut 1986; Hernquist 1987, 1990b) to calculate gravitational forces and smoothed particle hydrodynamics (SPH; Lucy 1977; Gingold & Monaghan 1977) to follow the evolution of the gas. Tree codes offer the best compromise for studies of merging galaxies, as they place no constraints on the symmetry of the system or on spatial resolution (other than that set by the gravitational smoothing length), while offering a very efficient $N \log N$ scaling of computing time. Gravitational forces are calculated using a tolerance parameter $\theta = 0.7$ and including terms up to quadrupole order in the multipole expansions. A cubic spline is used to soften gravitational forces (Goodman & Hernquist 1991), with different softening lengths for different species of particles. In the models described here, the softening lengths of the disk, bulge, and halo particles are $\epsilon_d = 0.08$, $\epsilon_b = 0.06$, and $\epsilon_h = 0.37$, respectively.

SPH is a Lagrangian technique in which the gas is partitioned into fluid elements represented by particles. These particles obey equations of motion similar to those for the collisionless particles, but with additional terms to describe pressure gradients, viscous forces, and radiative effects in the gas. The SPH particles have individual time steps chosen to satisfy the Courant condition (Monaghan 1992) with Courant number $C = 0.5$. A conventional form of the artificial viscosity is used (see, e.g., Monaghan & Gingold 1983; Monaghan & Lattanzia 1985), with parameters $\alpha = 0.5$, $\beta = 1.0$.

To optimize the spatial dynamic range of the code, SPH particles have their own smoothing lengths, such that a constant number $\mathcal{N}_s$ of neighbors are contained within two smoothing lengths. Estimates of the hydrodynamic variables are symmetrized to preserve momentum conservation, as described by Hernquist & Katz (1989). The choice of $\mathcal{N}_s$ represents a compromise between the goal of resolving smaller scales (small $\mathcal{N}_s$) and improved accuracy in the smoothed quantities (large $\mathcal{N}_s$). To reduce error propagation, we have chosen to smooth the hydrodynamic properties over $\mathcal{N}_s = 96$ neighbors. We note, however, that our results are in good agreement with earlier calculations that employed $\mathcal{N}_s = 30$ (see, e.g., Barnes & Hernquist 1991; Hernquist & Barnes 1994), indicating that the results are rather insensitive to the choice of $\mathcal{N}_s$.

We have opted to employ an isothermal equation of state for the gas with a temperature $T_{\rm gas} = 10^4$ K. Owing to limitations imposed by mass resolution with a finite number of particles, we are unable to describe a multiphase ISM (see, e.g., McKee & Ostriker 1977). As a result, earlier models that explicitly followed the radiative heating and cooling of the gas (see, e.g., Hernquist 1989) employed a cutoff temperature in the cooling curve at $T_c = 10^4$ K. Because of the short cooling time of disk gas, fluctuations in the gas temperature are quickly radiated away, so that most of the gas resides near this cutoff temperature. As a result, simulations with an isothermal equation of state differ little from those employing more "realistic" ones (Barnes & Hernquist 1995). Previous simulations have also shown that the hydrodynamic evolution of the ISM in mergers between disks and dwarf companions is quite robust against moderate changes in the equation of state (Hernquist & Mihos 1995). By choosing an isothermal equation of state for these models, we expedite the calculation with little cost in accuracy and simplify the interpretation of the results. However, the current models are insufficient to study fragmentation and star formation in tidal tails, as our models neglect adiabatic cooling which is important for rapidly expanding gas in the tidal debris.

The equations of motion are integrated using a time-centered leapfrog algorithm (see, e.g., Press et al. 1986). For the collisionless particles, a fixed time step of $\Delta t = 0.16$ is used for the bulgeless galaxies and $\Delta t = 0.08$ for galaxies that possess bulges. Scaled to values appropriate for the Milky Way (see § 2.3 below), these choices correspond to 2×10^6 yr and 10^6 yr, respectively. For our fiducial mergers, these time steps are reduced by a factor of 3 after the dense gas cores develop in the galaxies' centers in order to improve energy conservation. The SPH particles are allowed to have time steps smaller than the collisionless particles by powers of 2 in order to satisfy the Courant condition (Hernquist & Katz 1989). Because of the use of an isothermal equation of state and the effects of star formation (see § 2.2 below), energy is not strictly conserved in these calculations. However, based on previous calculations (Barnes & Hernquist 1995; Hernquist & Mihos 1995), integration errors are responsible for drifts in the total energy of only $\sim 0.1\%$ for the parameters employed.

2.2. *Star Formation Algorithms*

To model star formation, we use a variant of the Schmidt law (Schmidt 1959), which relates the star formation rate in disk galaxies to the local gas density by star formation rate (SFR) ($M_\odot$ yr^{-1} pc^{-3}) $\propto \rho_{\rm gas}^n$, where n has been determined empirically to lie in the range $1 \lesssim n \lesssim 2.5$ (see Berkhuijsen 1977; Kennicutt 1989 and references therein). Retaining the Lagrangian nature of SPH, we parameterize the star formation rate per unit mass in a gas particle according to $\dot{M}_{\rm gas}/M_{\rm gas} = C \times \rho_{\rm gas}^{1/2}$. Averaged over volume, this prescription yields an index $n = 1.5$ in the classical Schmidt law (Mihos & Hernquist 1994e). The constant of proportionality, C, is chosen such that an isolated disk galaxy forms stars at a rate of $\sim 1\ M_\odot$ yr^{-1}, yielding a depletion time for the disk of ~ 5.5 Gyr, similar to values inferred for present day disk galaxies (Kennicutt 1983).

We include the injection of energy into the ISM due to supernovae and stellar winds from massive stars ("feedback") by imparting kinetic energy to the surrounding ISM. At each time step, the total amount of energy released via massive star evolution $E_{\rm SN}$ is calculated from the star formation rate in each SPH particle, and a fraction $\epsilon_{\rm kin}$ of this energy is used to provide a radial "kick" to neighboring SPH particles. The magnitude of this kick is given by $\Delta v_i = [2(w_i \epsilon_{\rm kin} E_{\rm SN})/M_i]^{1/2}$, where i refers the neighbor being perturbed and w_i is an energy weighting based on the smoothing kernel (see Mihos & Hernquist 1994e). In order to limit the amount of kinetic energy injected into the ISM via star formation, we constrain $\epsilon_{\rm kin}$ so that the ISM in an isolated disk model maintains a constant vertical scale height with time. Tests employing isolated disk models indicate that $\epsilon_{\rm kin} = 10^{-4}$ provides good results in terms of the scale height of the disk gas and distribution of star formation (Mihos & Hernquist 1994e). Using $\epsilon_{\rm kin} = 10^{-4}$ and $E_{\rm SN} = 10^{51}$ ergs, Δv_i is typically

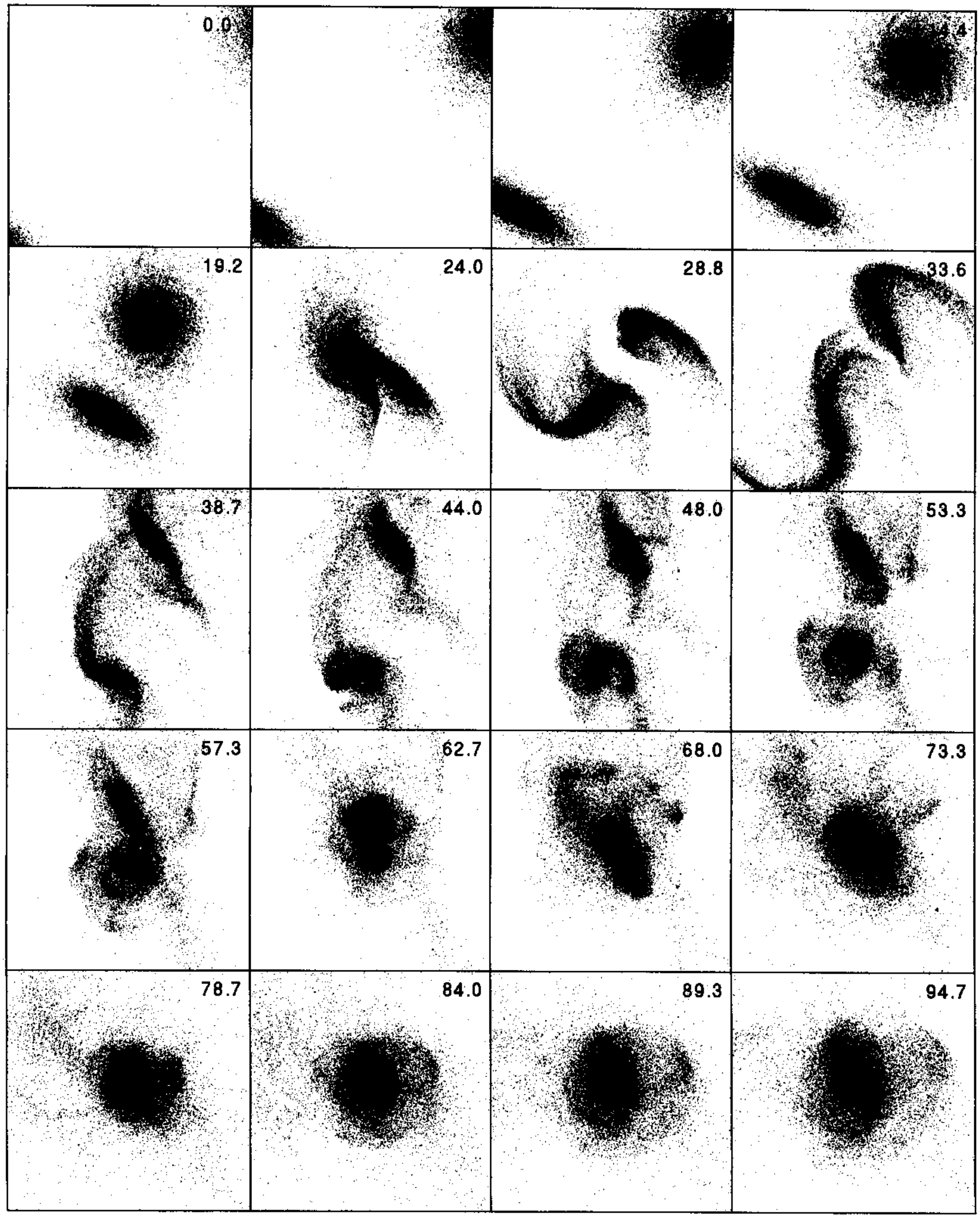

FIG. 1.—Evolution of the old stellar disk component in the fiducial disk/halo merger. The prograde disk enters from the upper right of the frames, while the inclined disk approaches from the lower left. Each frame measures 20 units on an edge; time is shown in the upper right-hand corner of each frame.

$\lesssim 0.1$ km s^{-1} for nearby neighbors, so that the *total* velocity perturbation in each star-forming particle is typically ~ 1 km s^{-1}. Concurrent with the energy release, star formation injects metals into the ISM, which allows us to track metallicity enrichment and to explore the development of gradients in the merger remnant.

To describe the effects of gas depletion and formation of a young stellar population, we employ a technique involving "hybrid" SPH/young star particles (Mihos & Hernquist 1994e) that are gradually converted from gaseous to collisionless form. We characterize these particles by both a total mass and a gas mass; the gravitational forces on and

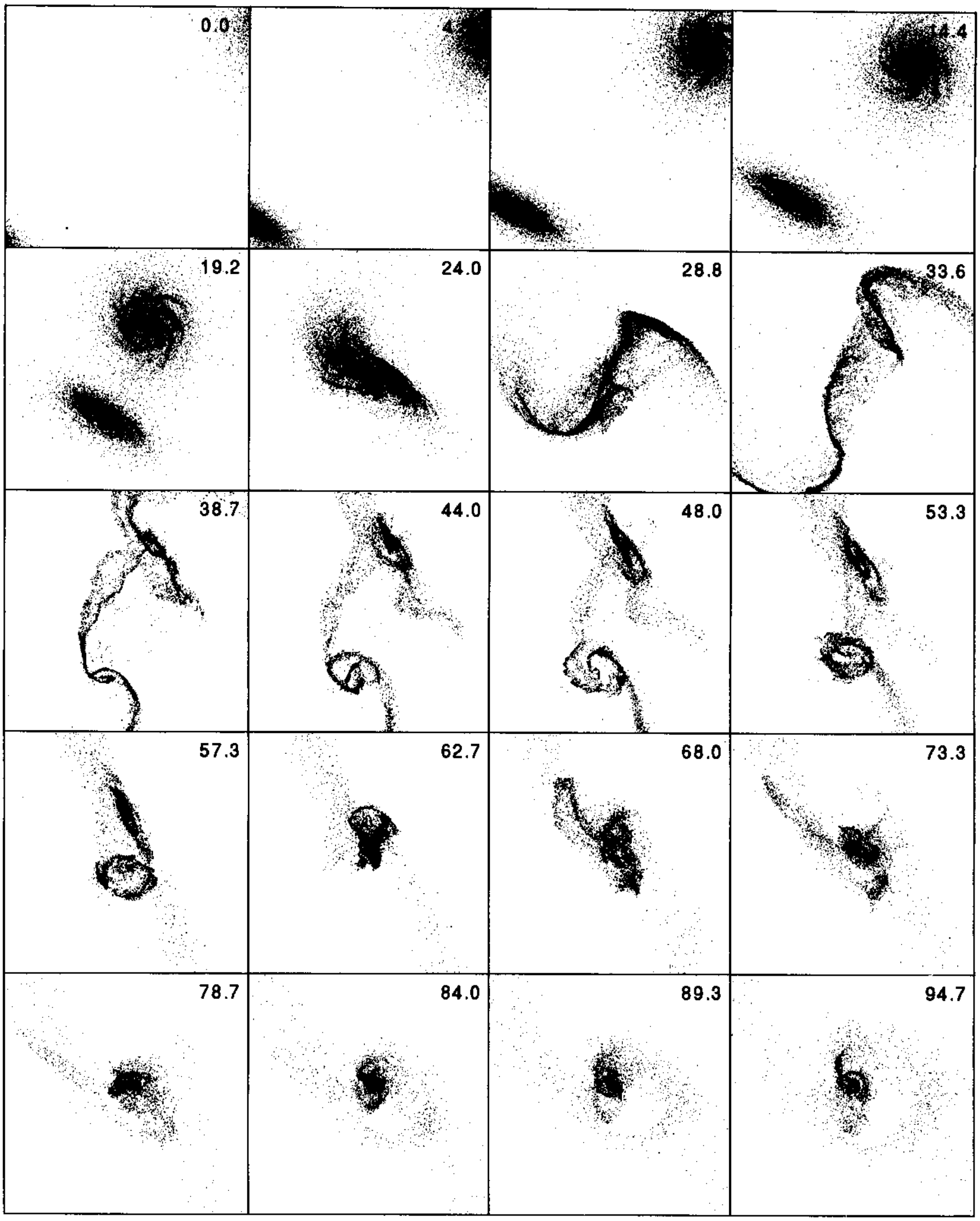

FIG. 2.—Evolution of the gas and young stellar components in the fiducial disk/halo merger. Scales as in Fig. 1.

acceleration of a hybrid particle are calculated using its total mass, while the gas mass is used to calculate the hydrodynamic forces and properties of the gas. Through star formation, the gas mass of a hybrid particle is reduced, while its total mass remains fixed, thereby mimicking the effects of gas depletion. When the gas mass fraction of a hybrid particle drops below 5%, it is converted to a collisionless particle, with its remaining gas mass smoothed out among its nearest neighbors. These converted particles thus act as a tracer of the young stellar population formed in a starburst event.

Our method of using hybrid particles to treat star formation and gas depletion has a number of computational advantages. The total number of particles remains fixed, which eliminates the need to invest computational resources in evolving large numbers ($N > 10^7$) of young star

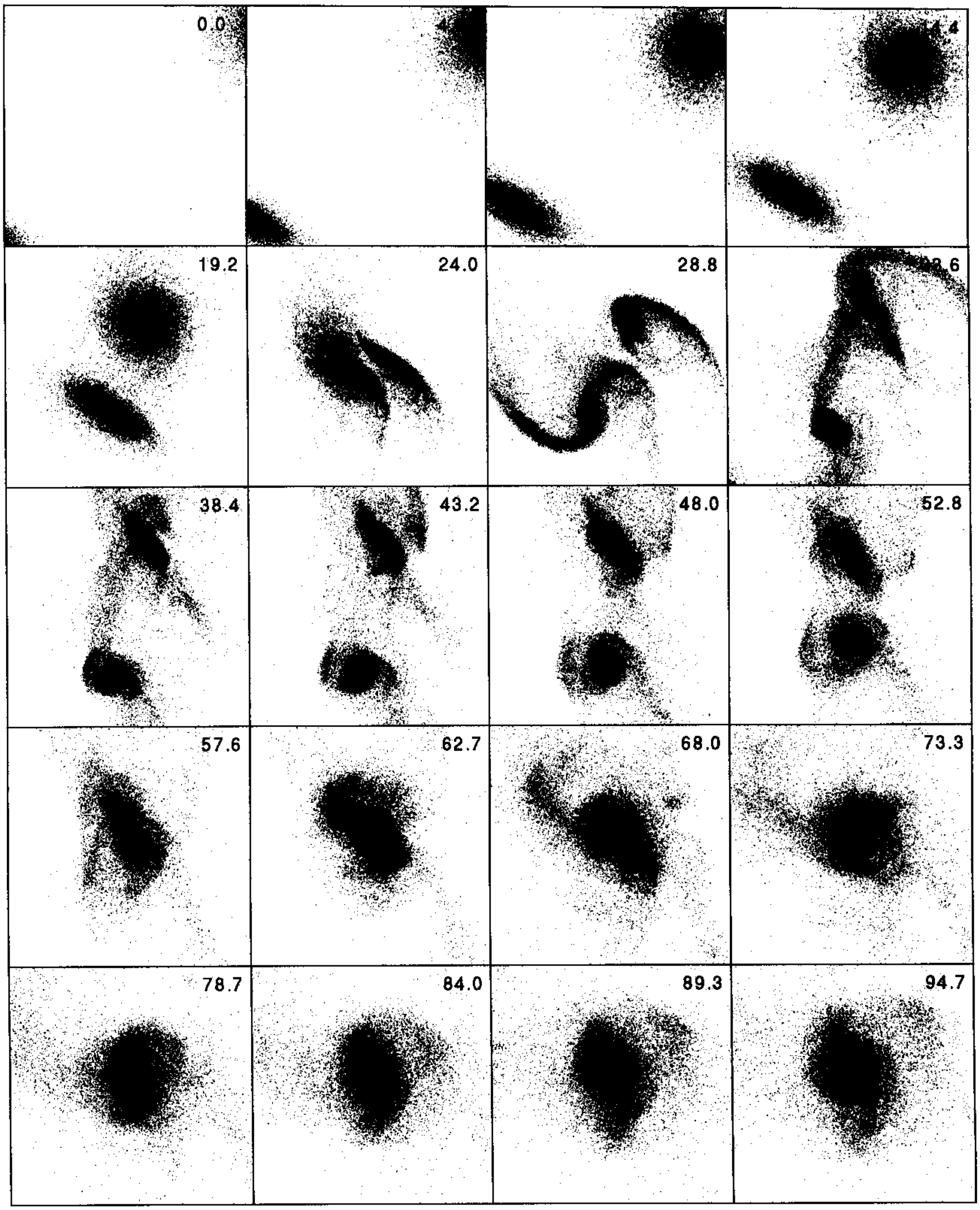

FIG. 3.—Evolution of the old stellar disk component in the fiducial disk/bulge/halo merger. Scales as in Fig. 1.

particles. Unlike methods that convert gas particles in toto (i.e., Summers 1993), our algorithm places no constraint on the conversion mass involved in a star formation event, allowing the models to describe the mass and time scales necessary to examine the detailed star forming properties of the system. The main disadvantage to our approach is that it assumes the newly formed stars and the parent gas are dynamically coupled until the gas is fully depleted. In reality, the two components will evolve separately, as the gas can experience shocks and dissipation, while the stars will evolve in a collisionless manner. This discrepancy will be greatest if, e.g., a shock passes through hybrid particles composed of roughly equal amounts of gas and stars. However, this discrepancy will be small if the hybrid particles are predominantly in one phase or the other, as is the case in starburst events, where gas is converted to stars over short timescales (i.e., less than the dynamical timescale, ~ 100 Myr). We believe, therefore, that the mass-weighted

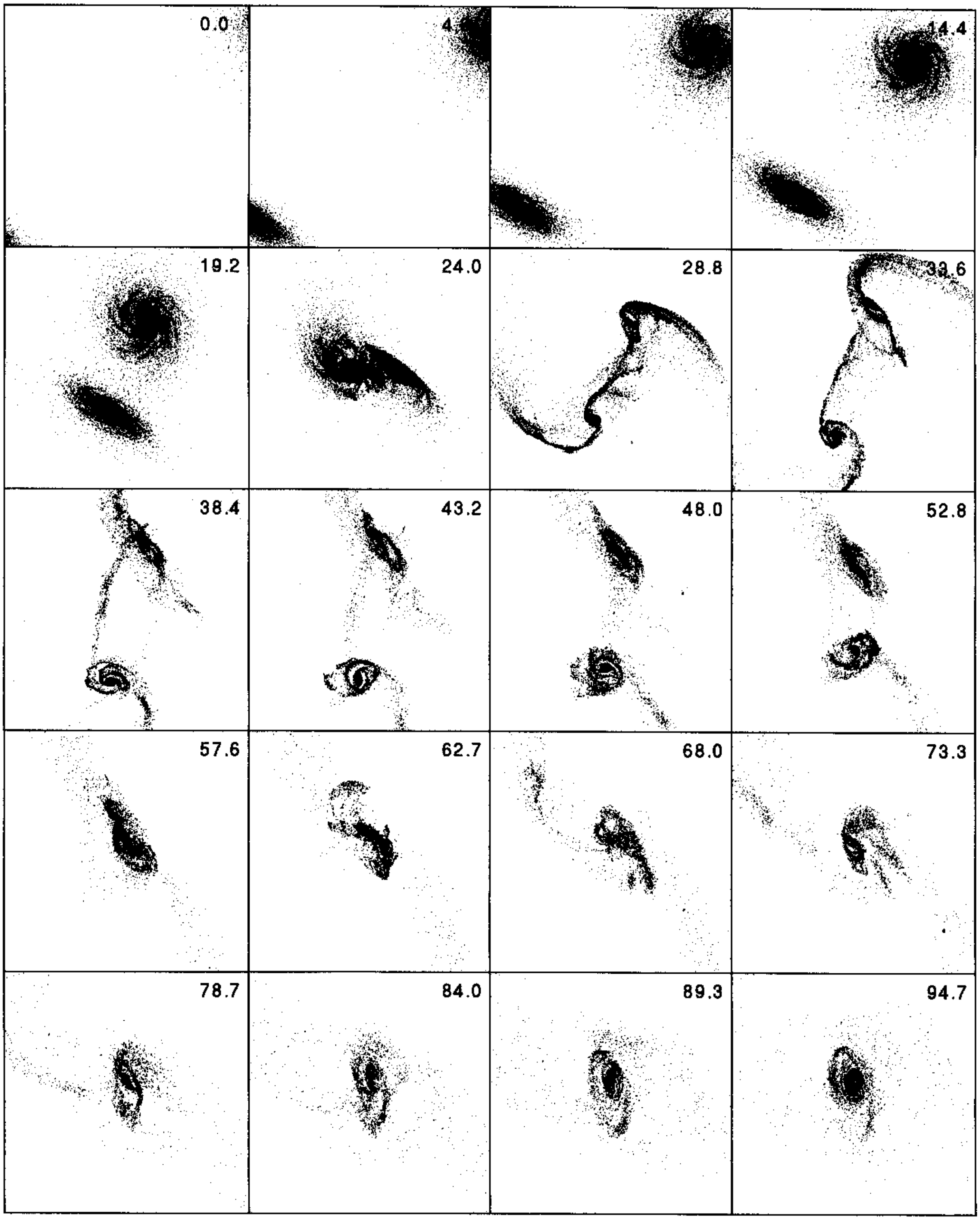

FIG. 4.—Evolution of the gas and young stellar components in the fiducial disk/bulge/halo merger. Scales as in Fig. 1.

error introduced by our method will be relatively small for the simulations presented here.

2.3. *Galaxy Models*

Our galaxy models are constructed using the technique described by Hernquist (1993b). The galaxies consist of a spherical "dark" halo, an exponential disk comprised of both stars and gas, and, optionally, a compact central bulge. The halo is modeled as a truncated isothermal sphere, the density of which is given by

$$\rho_h(r) = \frac{M_h}{2\pi^{3/2}} \frac{\alpha}{r_c} \frac{\exp(-r^2/r_c^2)}{r^2 + \gamma^2},$$

where M_h is the halo mass, r_c serves as a cutoff radius, γ is a "core" radius, and α is a normalization constant defined by

$$\alpha = \{1 - \sqrt{\pi}\, q \exp(q^2)[1 - \mathrm{erf}(q)]\}^{-1},$$

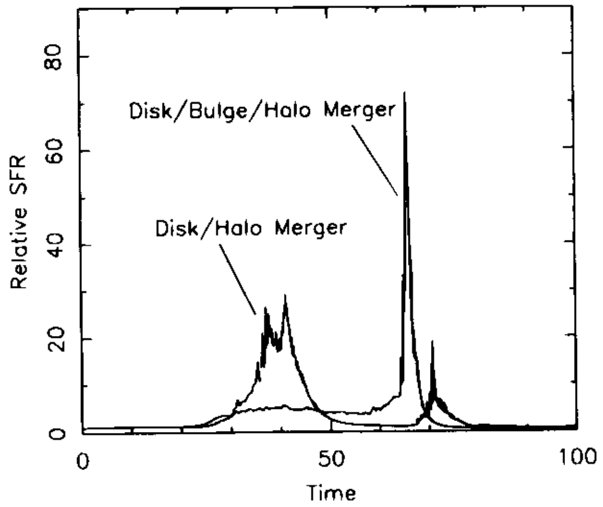

FIG. 5a

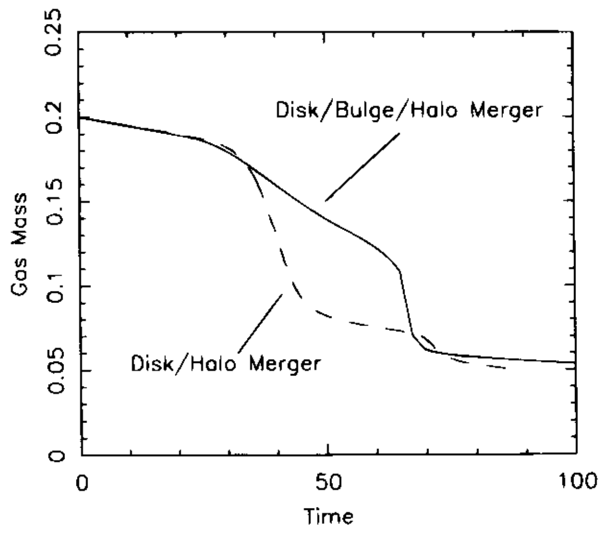

FIG. 5b

FIG. 5.—(a) Evolution of the global star formation rate (relative to two isolated disks) for the fiducial models. (b) Evolution of the total gas mass for the fiducial models.

where $q = \gamma/r_c$. The exponential stellar disks follow the density profile

$$\rho_d(R, z) = \frac{M_d}{4\pi h^2 z_0} \exp\left(-\frac{R}{h}\right) \mathrm{sech}^2\left(\frac{z}{z_0}\right),$$

where M_d is the disk mass, h is a radial scale length, and z_0 is a vertical scale thickness. The gas disks follow the same radial profile as the stellar disks but with a smaller vertical scale thickness, dependent on the gas temperature and galactic radius. In some models, we also include bulges, the density of which is given by an oblate generalization of the potential-density pair of Hernquist (1990a) for spherical galaxies and bulges:

$$\rho_b(m) = \frac{M_b}{2\pi a c^2} \frac{1}{m(1+m)^3},$$

where M_b is the bulge mass, a is a scale length along the major axis, c is a scale length along the minor axis, and

$$m^2 = \frac{x^2 + y^2}{a^2} + \frac{z^2}{c^2}.$$

Particles are distributed in space according to the density profiles outlined above, with velocities initialized using moments of the Vlasov equation and approximating the velocity distributions by Gaussians.

In the models described here, we use a system of units in which the gravitational constant $G = 1$, the disk mass $M_d = 1$, and the radial scale length of the disk $h = 1$. Scaling these values to those typical of the Milky Way (Bahcall & Soneira 1980; Caldwell & Ostriker 1981), unit length is 3.5 kpc, unit mass is $5.6 \times 10^{10}\ M_\odot$, unit velocity is 262 km s^{-1}, and unit time is $\sim 1.3 \times 10^6$ yr.

The galaxies are all characterized by halo and disk parameters $M_h = 5.8$, $\gamma = 1.0$, $r_c = 10.0$, and $z_0 = 0.2$. The stellar velocity dispersion in the disk is such that the Toomre Q parameter is normalized to 1.5 at the solar radius ($R_\odot = 8.5/3.5$) and varies only weakly with radius. In the models that include bulges, these bulges have mass $M_b = \frac{1}{3}$ and scale lengths $a = 0.2$ and $c = 0.1$. The numbers of collisionless particles associated with each component are $N_h = 32768$, $N_d = 32768$, and $N_b = 8192$. The disk gas, comprising 10% of the total disk mass, is represented by 16,384 hybrid SPH particles with an isothermal gas temperature of $T_{\rm gas} = 10^4$ K.

3. FIDUCIAL MODELS

In § 3 we concentrate on the evolution and star-forming properties of two fiducial galaxy mergers that differ only in the structure of the progenitor galaxies. We investigate the effect of varying encounter geometry in a wider, but less in-depth, analysis of merger simulations in § 4.

Our fiducial models involve two identical, equal-mass disk galaxies colliding on a nearly parabolic orbit that leads to rapid merging over a few disk rotation periods. The galaxies are initially placed at a separation of $r_{\rm init} = 30$, and at first close passage the pericentric separation (for the ideal Keplerian orbit) would be $r_{\rm peri} = 2.5$. The geometry of the encounter is described by the inclination of the disks relative to the orbital plane (i_1 and i_2) and their argument of periapse (ω_1 and ω_2) (see, e.g., Toomre & Toomre 1972). Our fiducial mergers involve one exactly prograde galaxy ($i_1 = 0°$, ω_1 undefined) and one highly inclined galaxy ($i_2 = 71°$, $\omega_2 = 30°$). The two fiducial models employ different galaxies: in the first case (referred to as the "disk/halo" model), the galaxies are both composite disk/halo galaxies lacking a bulge component, while in the second case (the "disk/bulge/halo" model), both galaxies also possess dense bulges with a bulge:disk mass ratio of 3:1.

3.1. *Dynamical Evolution*

Figure 1 shows the evolution of the old stellar component in the fiducial disk/halo galaxy merger.[4] Shortly after their initial close approach at $t \sim 24$, the galaxies become severely distorted, forming long tidal tails and a bridge connecting the two galaxies. In response to the tidal force from the passing companion, the inner regions of each disk also form linear barlike structures. The galaxies continue to separate after the initial passage; however, the dark matter halos of the galaxies are "spun up" by the encounter, because of an

[4] In what follows, we refer to the collisionless particles originally comprising the exponential disk as the "old stellar component" and refer to the stars formed via star formation as the "young stellar component."

efficient conversion of orbital angular momentum into internal spin (Barnes 1992; Hernquist 1992, 1993a). As a result, the galaxies brake on their orbit, achieving a maximum separation of $r_{\rm apo} \sim 12$ before turning around and falling back together.

As the galaxies encounter one another again, they experience a second quick passage, with $r_{\rm peri} \sim 1.5$ and $r_{\rm apo} \sim 2.5$, before finally merging at $t \sim 65$. Violent relaxation transforms the stellar component into a distribution that possesses an $r^{1/4}$ law surface density profile over a large range in radius (Barnes 1992; Hernquist 1992, 1993a). Irregular structure in the inner regions is rapidly mixed away, which leaves a remnant that resembles—at least superficially—an elliptical galaxy. At large radii (i.e., $r > 3$), where the dynamical timescale is much longer, irregular structures such as shells, plumes, and tails persist; this "fine structure" may provide a long-lived signature of the merger in the remnant galaxy.

While the stellar component in each galaxy follows a collisionless evolution, the gaseous components, shown in Figure 2, are subjected to strong shocking and dissipation of energy and angular momentum and evolve in a distinctly different manner. During the initial close passage, gas shocks at the interface between the two galaxies and forms a physical bridge between them as they begin to separate (see $t = 28.8$). At first, the gas in the disks responds much like the stars, but the response in the gas is sharper as it crowds along the stellar bars. The nonaxisymmetric potential of the distorted disks acts to torque the disk gas (see § 3.3), driving a rapid radial inflow of gas—by $t = 48$, approximately half of all the gas has been driven into the inner few hundred parsecs of the galaxies, where it fuels intense starburst activity (§ 3.2).

As the galaxies approach the final stages of merging, the rapidly changing gravitational potential forces much of the remaining gas onto intersecting orbits, where it shocks, dissipates energy, flows to the center of the remnant, and forms stars. By the time the merger is complete, approximately three-quarters of the gas originally in the disks ends up in a compact starburst core at the center of the remnant (Mihos & Hernquist 1994c). Most of the remaining gas has settled into a warped, diffuse disk at intermediate radii, with a small fraction of gas remaining at large radii in the tidal tails, where it will continue to rain back in on the remnant over many gigayears.

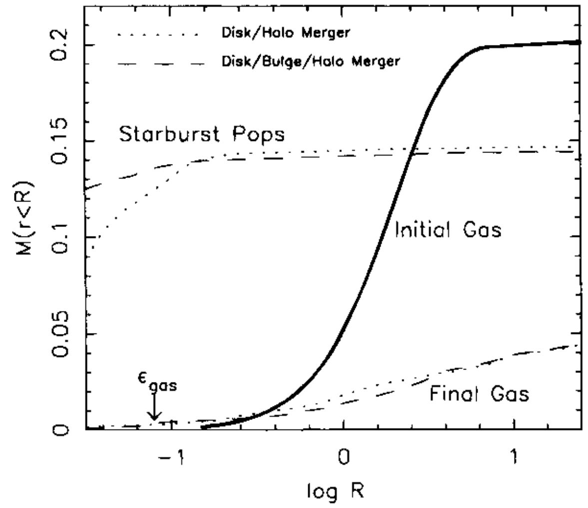

FIG. 6.—Comparison of the initial and final cumulative mass distributions of gas and young stars in the fiducial mergers. Note the compact starburst cores and the increasing amount of gas at larger radii in the merger remnants.

To illustrate the consequences of varying the internal structure of the merging galaxies, Figure 3 shows the evolution of the old stellar component in a merger involving galaxies with compact central bulges. Because the bulges comprise only $\sim 5\%$ of the total dynamical mass of the galaxies, the global evolution of this simulation is very similar to the fiducial disk/bulge merger. The important difference lies in the response of the inner disk; rather than forming a strong bar after the initial collision, the disk sports features more reminiscent of two-armed spiral patterns (see $t = 33.6$). These structures are less effective at driving gaseous inflows in the disk than bars; thus, while gas flows inward in each galaxy, it does so only slowly and settles into a quasi-steady state before reaching the center. As a result, the distribution of gas in the central regions of the galaxies is much more diffuse than in the disk/halo mergers, as suggested by Figure 4; the star formation rate is elevated only modestly during this portion of the evolution, and the gas is not greatly depleted.

When these disk/bulge/halo galaxies finally merge, strong gravitational torques deprive the gas of nearly all of its angular momentum, driving it into the central regions of the remnant. In only $\sim$20–30 Myr, over half the remaining gas in the system settles into a massive "cloud" a few hundred parsecs in diameter. The high gas densities in this cloud fuel an intense starburst, creating a compact, young population of stars in the center of the remnant. Although the history of dissipation and star formation is very different in our two fiducial simulations, the net conversion of gas into young stars is remarkably similar—about 75% of the gas is depleted in each case. As for the disk/halo merger, the remaining gas in the disk/bulge/halo remnant is either distributed in a warped gas disk at intermediate radii or lies at much greater distances in the tidal tails. Again, infall of gas from the tidal features continues over long timescales.

3.2. *Star Formation*

The star-forming response of the galaxies during the fiducial mergers has been described elsewhere (Mihos & Hernquist 1994b); here, we describe this aspect of the simulations only briefly. We note again that our star-forming prescription is the density-dependent Schmidt law, such that peaks in the modeled star formation rate indicate periods of strong inflow and peaks in gas densities in the galaxies. While the use of a Schmidt law in the extreme central environments of merging galaxies may be a suspect parametrization, it should at least give an estimate of the onset and timescale for the induced starburst activity. However, predictions of absolute levels of star formation will carry significant uncertainties.

In the disk/halo mergers, early dissipation and inflow produce central starbursts in the disks shortly after their initial encounter, when the galaxies are still widely separated, as can be inferred from the star formation rates shown in Figure 5*a* (see Mihos & Hernquist 1994b for images). The star formation rates (SFRs) in each disk peak at 20–30 times their initial amplitude, with an order-of-magnitude increase sustained for $\sim$150 Myr. As these starbursts deplete the nuclear regions of gas (Fig. 5*b*), the starbursts die out, and the global SFR declines to its pre-encounter level well

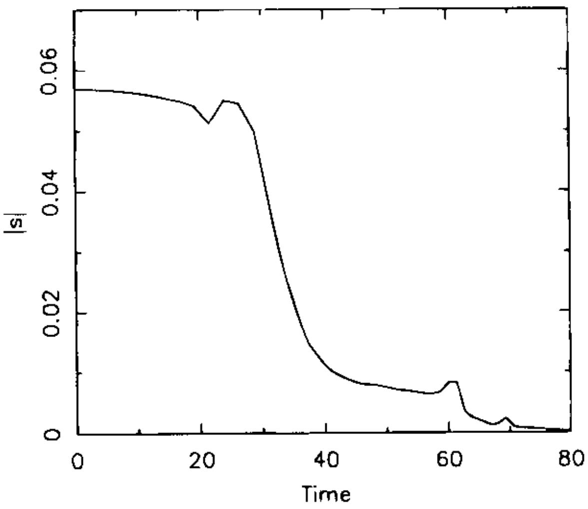

FIG. 7*a*

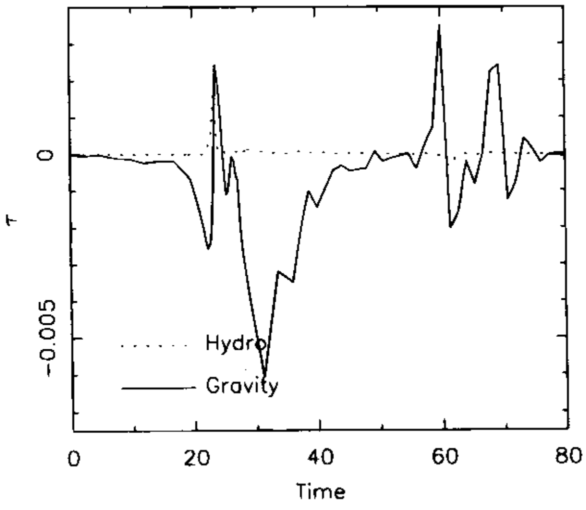

FIG. 7*b*

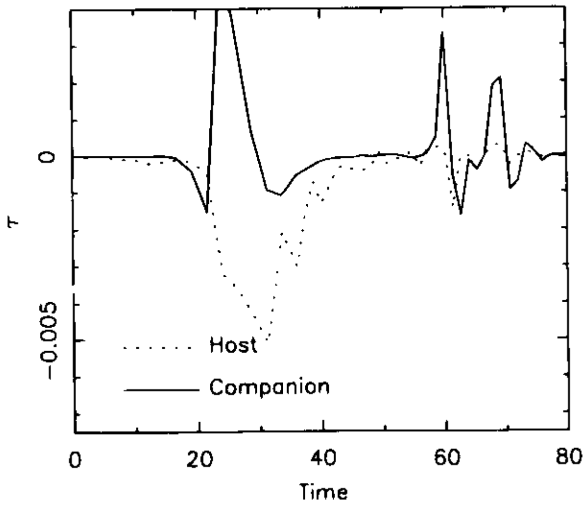

FIG. 7*c*

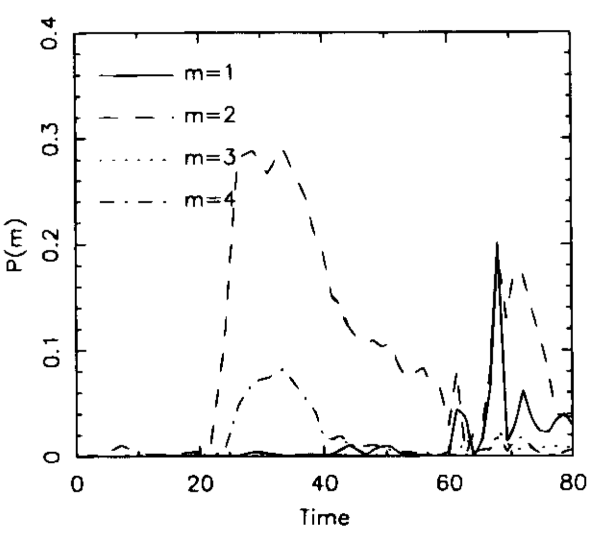

FIG. 7*d*

FIG. 7.—Angular momentum and torque decomposition for the gas in the prograde disk/halo galaxy. (*a*) Spin angular momentum. (*b*) Gravitational and hydrodynamical torques. (*c*) Gravitational torques from each galaxy. (*d*) Fourier modal analysis of the stellar prograde disk.

before the galaxies merge. Dissipation during the final stages of the merger fuels a relatively weak starburst in the center of the remnant,[5] which rapidly fades. Continued infall of gas from the tidal tails is not sufficient to fuel significant levels of further star formation, and the remnant evolves passively thereafter.

The merging disk/bulge/halo galaxies have a much different star-forming history. Because the spiral response of the disks to the interaction is much less effective at driving gaseous inflows than bars, the starbursts that develop after the initial encounter are much weaker in strength than those in the bulgeless galaxy mergers. The global SFR is increased by only a factor of a few during the intermediate stages of the interaction (Fig. 5*a*), and the disk gas is not significantly depleted (Fig. 5*b*). Consequently, when the galaxies finally do coalesce, they have fully twice the gas mass remaining as their bulgeless counterparts, and the rapid collapse of this gas drives a furious starburst at the center of the merging system. To the extent that a Schmidt law is valid, the SFR peaks at more than ~ 70 times its preinteraction rate, and the rapid gas depletion burns the starburst out after only ~ 50 Myr. It is important to note that the relative SFR shown in Figure 5*a* is defined with respect to its preinteraction value in the galaxy *pair*; because the starburst triggered in the disk/bulge/halo merger occurs in one merged object, the factor of ~ 70 increase in relative SFR corresponds to a rate that is nearly 150 times larger than that in a *single* isolated disk galaxy. Again, once this starburst dies out, the remnant evolves only passively in terms of its star forming properties.

It is interesting to note that while the fiducial models have very different star-forming histories, their *time-integrated* star-forming properties are quite similar. In both cases, approximately 75% of the original disk gas is converted into stars, leaving behind a dense stellar core in the center of the remnant (Fig. 6; see also Mihos & Hernquist 1994c). While a significant fraction of gas is launched to

[5] We note a discrepancy between Fig. 5 and the similar Fig. 2 of Mihos & Hernquist (1994b). Because of the relatively coarse time steps used by Mihos & Hernquist (1994b), the dynamics of material near the dense cores was somewhat compromised. Our new more careful (and costly) simulation corrects that problem; however, while some small quantitative differences exist, the overall conclusions of Mihos & Hernquist (1994b) remain unchanged. We comment further on this issue in § 4.1.

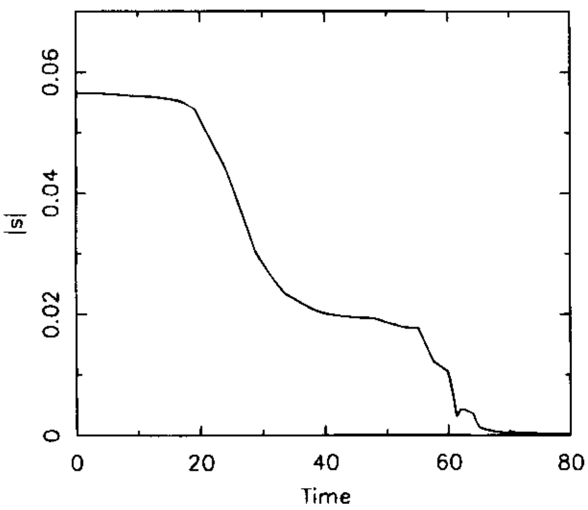

FIG. 8a

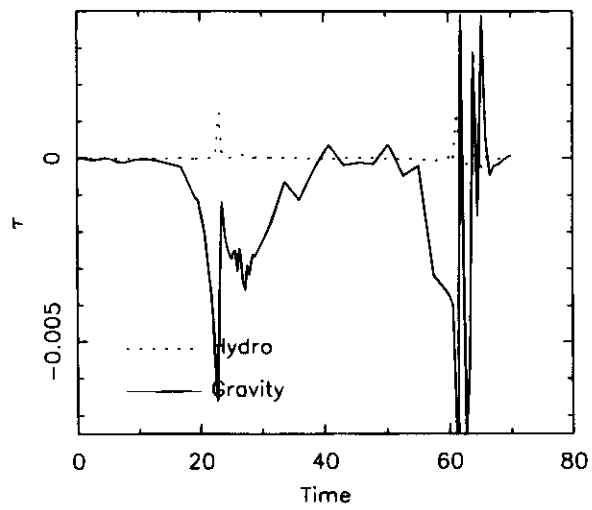

FIG. 8b

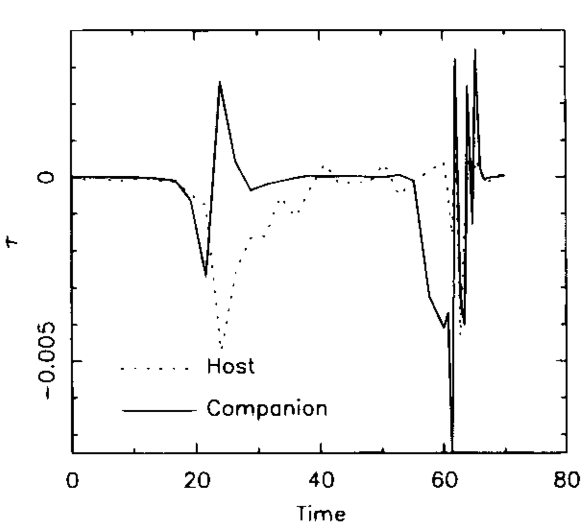

FIG. 8c

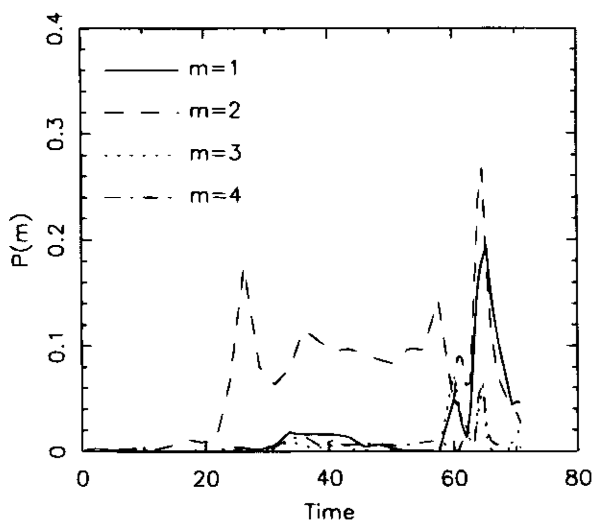

FIG. 8d

FIG. 8.—Angular momentum and torque decomposition for the gas in the prograde disk/bulge/halo galaxy. (*a*) Spin angular momentum. (*b*) Gravitational and hydrodynamical torques. (*c*) Gravitational torques from each galaxy. (*d*) Fourier modal analysis of the stellar prograde disk.

great distances in the tidal tails, an easily detectable amount of cold gas remains in the remnant ($\sim$a few $\times\ 10^9\ M_\odot$). This gas mostly lies in a warped, diffuse disk, similar to the H I disk seen in the peculiar elliptical galaxy NGC 5128 (Cen A; van Gorkom et al. 1990; Schiminovich et al. 1994). We also note the presence of small star-forming clumps of gas and stars in the tidal tails; while the gasdynamics of the tails is somewhat compromised by the use of an isothermal equation of state for the gas, star-forming objects like these have been seen in the tails of merger candidates such as NGC 7252 (Schweizer 1982), NGC 4038/39 (Mirabel et al. 1992), Arp 105 (Duc & Mirabel 1994), and the "Superantennae" (IRAS 19254−7245; Mirabel, Lutz, & Maza 1991). It seems clear from these models that the combined effects of dissipation and star formation should leave behind long-lived signatures of the merging process that may potentially be used to identify present-day galaxies as products of mergers.

3.3. *Gas Inflow*

To identify the mechanisms responsible for the inflows in the merging galaxies, we first isolate the gas that suffers the

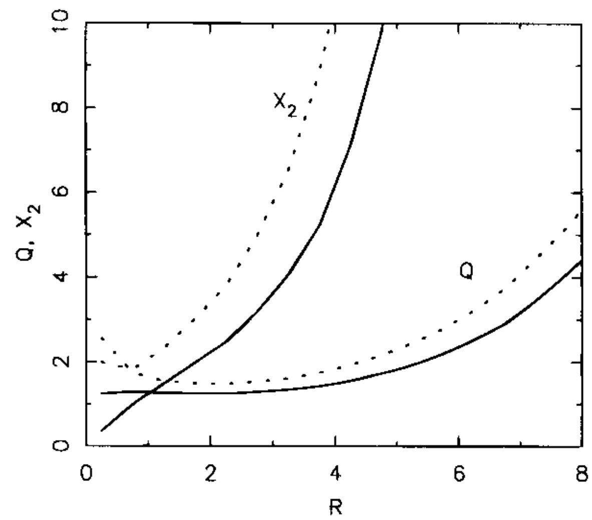

FIG. 9.—Disk stability parameters Q and X_2 in the disk/halo galaxy model (*solid curves*) and disk/bulge/halo galaxy model (*dashed curves*).

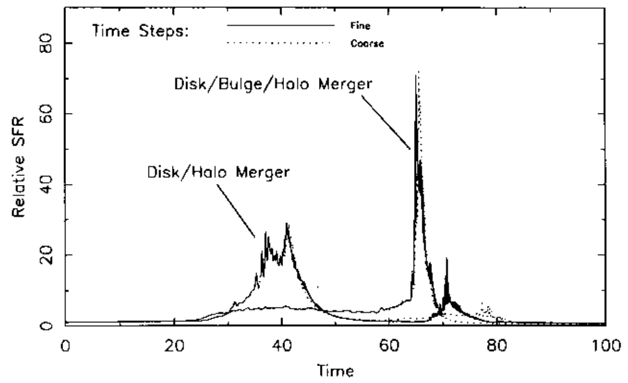

FIG. 10.—Comparison of the star formation rates in the fiducial models with and without the use of refined time steps. Solid lines show the response of the models that employ refined time steps, while dotted lines show the response of the models with the coarser time steps.

greatest loss of angular momentum and then decompose the time-dependent torques acting on these particles. Owing to star formation, which converts gas into stars, this material is more correctly a "gas + young star" mass; however, since the starburst population is born only when the inflow has mostly run its course, these particles are predominantly gaseous during the period of greatest loss of angular momentum. In this section, therefore, we will speak of angular momentum and torques acting on the *gas*, but the reader should bear in mind that the matter being tracked in the analysis is actually the hybrid gas/young star particles.

The first step is to identify all gas/young star particles in the central clump (at $r < 0.1$, or $\lesssim 350$ pc) of the merger remnant at late times. In each fiducial model, this mass amounts to $\sim 75\%$ of the initial gas content of the disks. Because we are interested primarily in the evolution of the *spin* angular momentum of the gas (to identify inflows in the disks), we exclude particles that fell in late from the tidal tails or that were transferred to the companion galaxy at intermediate times.[6] This cut, which removes $\sim 20\%$ of the particles in the central clump, allows for a much cleaner estimate of the spin angular momentum and torques acting on the bulk of the gas in each galaxy. The final subset of gas particles used in the analysis comprises 59% (disk/bulge merger) or 56% (disk/bulge/halo merger) of the initial gas content of the disks.

Figure 7*a* shows the evolution of the spin angular momentum of the gas in the prograde disk of the fiducial disk/halo galaxy merger. At closest approach, $t \sim 24$, the spin increases slightly as angular momentum is transferred from the orbital motion of the galaxies to the internal spin of the disks, and the tidal tails are formed. Shortly thereafter, the gas rapidly dissipates energy and loses angular momentum, as it shocks along the bar, and flows inward toward the galaxy center. In the inclined disk, the response is similar, although differences resulting from the geometry are apparent. In particular, gas in the inclined disk loses less angular momentum than gas in the prograde disk; however, these differences are small, and strong inflow develops in the inclined disk as well.

These inflows rapidly transport gas to the inner regions of the disks. By $t = 48$, when the galaxies are still widely separated, $\sim 80\%$ of the material that ultimately ends up in the remnant core has already collapsed to within $r < 0.1$ (350 pc) of its host galaxy's center. When the galaxies merge at $t \sim 65$, these dense cores coalesce in a mostly collisionless manner (since the gas has largely converted to young stars); a small amount of the remaining gas is driven to the remnant center to complete the era of strong dissipation in the merger.

To identify the factors responsible for the gas inflow in the prograde galaxy, we decompose the torques acting on the gas. Figure 7*b* shows the gravitational and hydrodynamical torques. The latter are always small, except during the initial collision, when they *add* spin angular momentum to the gas, as found also by Barnes & Hernquist (1995). At later times, when the galaxies are finally merging ($t \sim 65$), hydrodynamic torques are also small, at least partly because of the fact that the gas has largely been converted to stars by that time. The gravitational torques are strongest during the period $t \sim 25$–40, corresponding to the times of most rapid inflow. When the galaxies merge, the rapidly varying gravitational potential acts to strongly torque the gas/young star population, driving an additional small inflow towards the center of the remnant.

Figure 7*c* further decomposes the gravitational torques into those from the host galaxy and those from the merging companion. The companion mainly *spins up* the gas on successive passages (i.e., $t \sim 24$, 60), acting against the inflow. In fact, the gravitational torques from the host galaxy itself are mostly responsible for the inflow, and a Fourier analysis of the old stellar component of the disk (Fig. 7*d*) shows that these torques coincide with the growth and strength of the $m = 2$ mode in the stellar disk. During the final merger, the companion acts as both a sink and a source for angular momentum, but the host galaxy primarily drives the inflow. At these late times, however, the modal analysis becomes ill defined, as violent relaxation largely destroys the disk of the galaxy.

This analysis confirms quantitatively the picture outlined in § 3.1. During the initial collision, gravitational torques from the companion spin up the prograde disk, forming the tidal tails and triggering the growth of a strong $m = 2$ bar mode in the disk. The response of the stars and gas to the perturbation is slightly different, as the gas bar tends to lead the stellar bar by a few degrees (Barnes & Hernquist 1991). The segregation of stars and gas along the bar allows the stellar bar to torque the gas gravitationally and initiate a rapid inflow while the galaxies are still widely separated. A powerful central starburst ensues, which rapidly depletes the galaxies of a large fraction of their ISM. When these galaxies finally merge, the rapidly varying gravitational torques drive a small additional amount of gas toward the center, fueling a weak starburst.

A similar analysis of the prograde disk in the disk/bulge/halo merger, shown in Figure 8, provides an interesting contrast to the evolution detailed above. Unlike the rapid, early loss of spin angular momentum by the gas seen in the disk/halo merger, the gas in the disk/bulge/halo merger experiences a two-stage dissipational history, as can be inferred from Figure 8*a*. The gas sheds $\sim 60\%$ of its initial spin angular momentum shortly after first close approach, but the inflow is retarded at $t \sim 35$ as the inflowing gas reaches a new dynamical equilibrium. This state is disrupted when the galaxies finally merge, which triggers a second period of strong inflow during which the massive gas

[6] For a discussion of the evolution of the *total* angular momentum of the gas, see Barnes & Hernquist (1995).

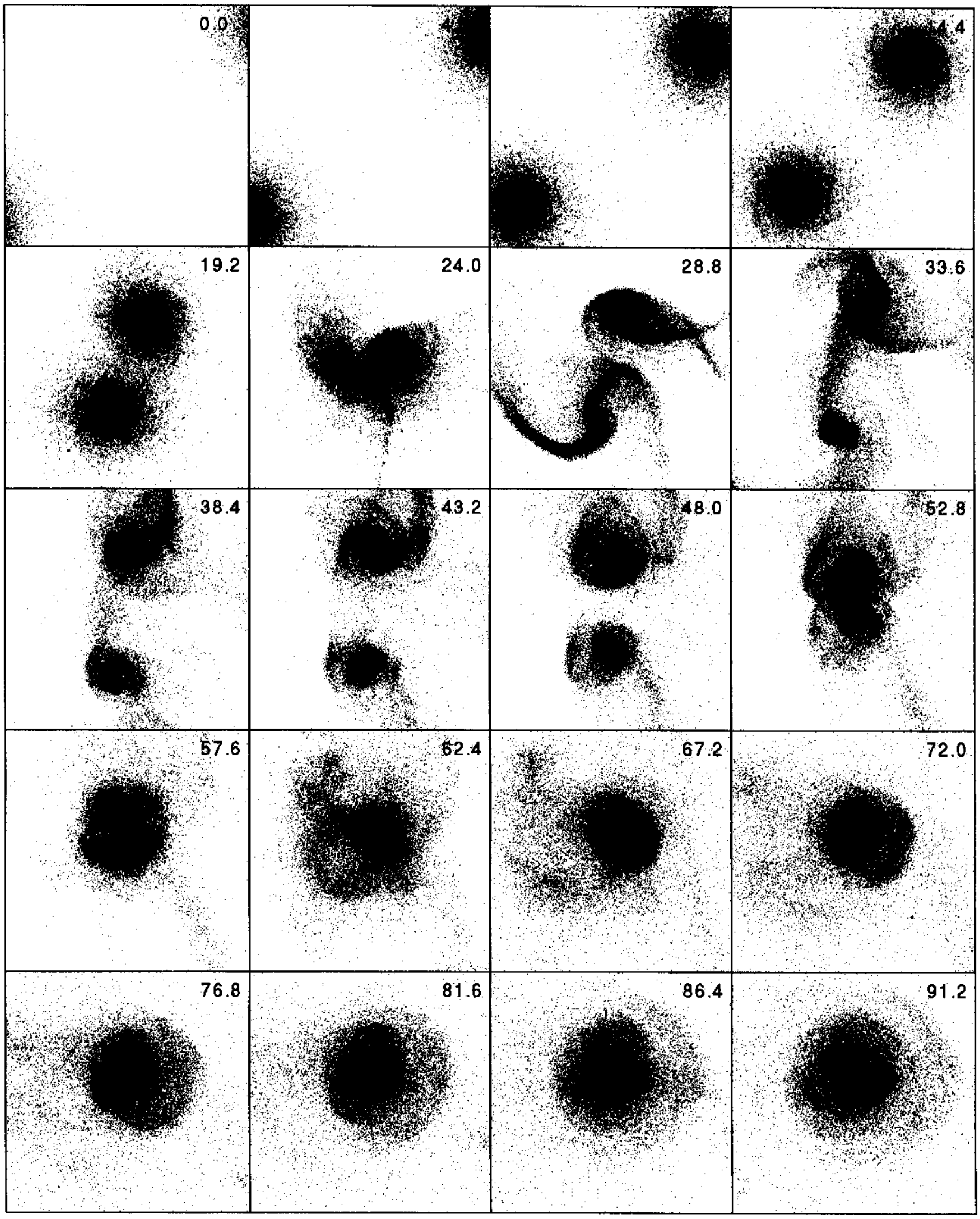

FIG. 11.—Evolution of the old stellar disk component in the prograde-retrograde disk/halo model. The prograde disk enters from the upper right of the frames, while the retrograde disk approaches from the lower left. Scales as in Fig. 1.

cloud forms in center of the remnant, fueling a violent starburst.

The torque decomposition shown in Figure 8*b* again demonstrates that hydrodynamic torques, important only when the galaxies are physically in contact with one another, tend to *add* angular momentum to the gas, while the gravitational torques are responsible for the inflow. The first inflow is again driven largely by the host disk; however, a comparison of Figures 8 and 7 shows that the torques are weaker in the disk/bulge/halo galaxies, which results in a less violent response. The relative weakness of these torques is directly attributable to the milder reaction of the stellar disk to the encounter. Figure 8*d* shows a Fourier analysis of the mass density of the stellar disk; while the $m = 2$ mode is clearly visible, it is reduced in strength compared to that in the fiducial disk/halo model, as the response of this disk is

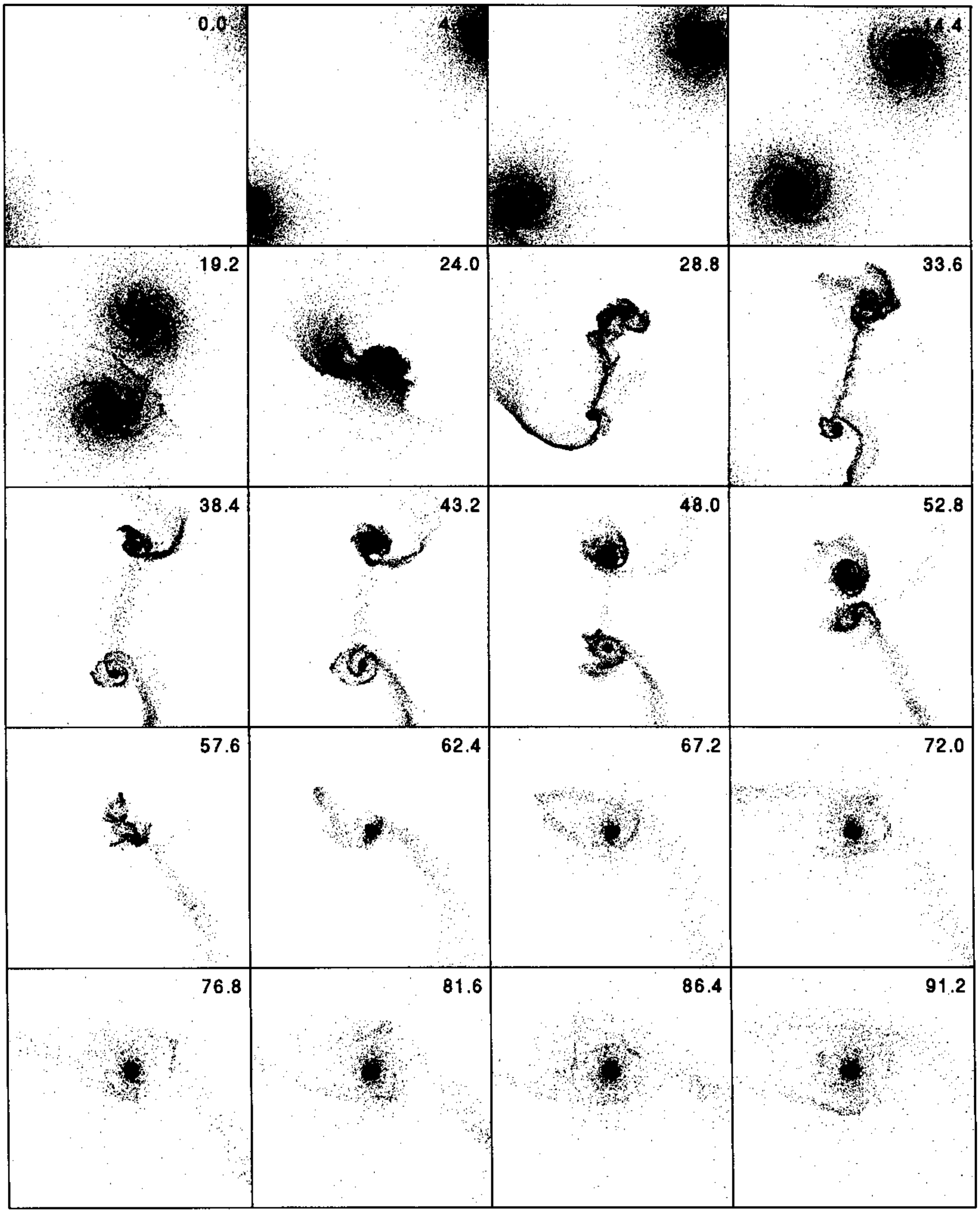

FIG. 12.—Evolution of the gas and young stellar components in the prograde-retrograde disk/halo model. Scales as in Fig. 1.

more in the fashion of a two-armed spiral rather than a strong linear bar mode. When the galaxies finally do merge, gravitational torques from both galaxies act to drive the gas into the center of the remnant.

What causes the different responses of the stellar disks in the different galaxy models? Figure 9 shows a plot of the disk stability parameters Q (Toomre 1962) and X_2 (Toomre 1981). In both models, $Q > 1$ over the entire disk, ensuring that the disk does not suffer from local axisymmetric instabilities. However, the X_2 parameter, which measures the stability of disks to the growth of global $m = 2$ modes, is markedly different in the inner regions of the two models. In the disk/halo model, $X_2 < 1$ over the inner scale length of the galaxy, showing that the disk is susceptible to strong amplification of any $m = 2$ perturbation. As a result, this disk responds more violently to the companion's tidal field, driving the gas inward early in the interaction. By contrast, the inclusion of a dynamically hot bulge component in the

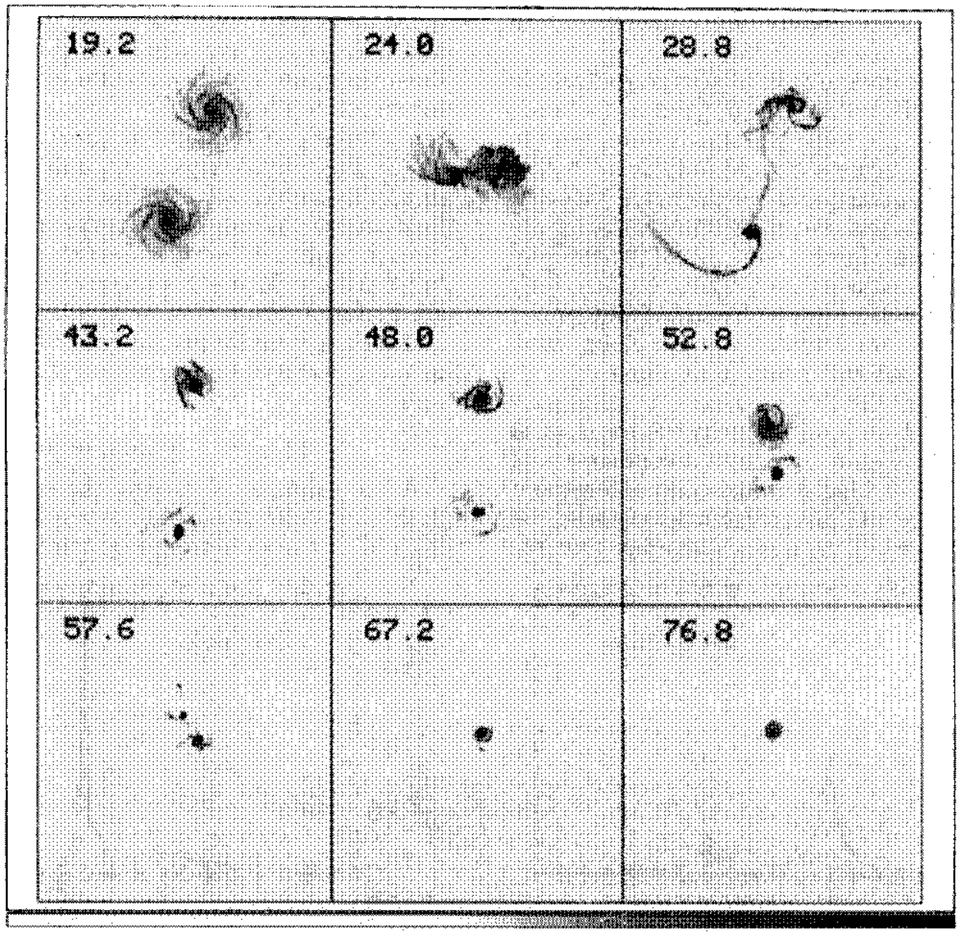

FIG. 13.—Evolution of the star-forming morphology of the prograde-retrograde disk/halo model. Because of the use of a density-dependent Schmidt law, this figure is comparable to a map of local gas density. A logarithmic intensity map is used to best show faint detail. Scales as in Fig. 1.

disk/bulge/halo galaxy model stabilizes the inner regions of the disk against the growth of $m = 2$ modes, which results in a weaker response to the perturbation of the companion. As shown by the torque analysis, this weaker $m = 2$ mode is less effective at driving an inflow, and early starbursts are inhibited in these galaxies.

In essence, therefore, we have a description of gas inflow and starbursts in mergers in which those effects are at least partly regulated by the internal structure of the merging galaxies. Galaxies that lack central bulges to stabilize them against $m = 2$ structures respond violently after the initial collision, forming a strong central bar. This bar acts to drives gaseous inflow early in the encounter, which gives rise to starburst activity while the galaxies are still widely separated. These early starbursts quickly deplete the gas, so that when the galaxies finally merge, they are relatively gas poor and suffer only weak starbursts. By contrast, the inclusion of a compact central bulge stabilizes the galaxies against the development of strong bars and inhibits early inflow and starburst activity. When these gas-rich galaxies merge, the strong gravitational torques drive the gas to the center of the remnant and fuel an intense but very short-lived starburst.

4. VARIED GEOMETRIES

To assess the role played by encounter geometry in fueling inflow and starburst activity, we have run other models similar to the fiducial mergers described in § 3, but with varying disk inclinations. As in the fiducial models, these encounters all involve equal mass galaxies colliding on initially parabolic orbits with $r_{\rm init} = 30$ and $r_{\rm peri} = 2.5$. While the fiducial models followed a prograde-inclined collision ($i_1 = 0°$, ω_1 undefined; $i_2 = 71°$, $\omega_2 = 30°$), these additional models involve a prograde-prograde collision ($i_1 = 0°$, ω_1 undefined; $i_2 = 0°$, ω_2 undefined), a prograde-retrograde collision ($i_1 = 0°$, ω_1 undefined; $i_2 = 180°$, ω_2 undefined), and an inclined-inclined collision ($i_1 = 71°$, $\omega_1 = -30°$; $i_2 = 71°$, $\omega_2 = 30°$). For *each* choice of geometry, we ran one simulation involving two bulgeless galaxies and one simulation involving galaxies with central bulges, with a bulge:disk mass ratio of 1:3. While this set of eight models is not an exhaustive survey of encounter parameters, the calculations allow us to explore the robustness of some of our claims based on the fiducial models.

4.1. *Time Step Concerns*

Because of the great computational cost of our simulations, the extra simulations were run without refining the time step by a factor of 3 when the dense clouds of gas developed in the galaxies, as was done for the fiducial models of § 3. Using the coarser time step throughout the simulation reduced the CPU requirements considerably. There is a price to pay for this compromise, however; at late times in the calculation, when dense gaseous cores form in the galaxies' centers, the use of a coarser time step entails a poor integration of the orbits of particles near these gas clumps. In particular, energy conservation is degraded, with total energy drifts amounting to $\sim 10\%$.

How does this loss in computational accuracy affect the results? In large part, the errors are confined to the inner regions of the galaxies, where the gas clouds dominate the dynamics. For example, models that include dense bulges experience a "numerical scattering" of the bulge particles, which artificially lowers the central stellar density of the galaxies after they merge. However, the *global* dynamics of the merger are mostly unaffected, as we have confirmed by comparing the fiducial simulations with and without refined time steps. Accordingly, our claims about the global morphology and stellar and gas kinematics seem sound.

Of greater concern are the consequences for the triggering of gas inflows and starburst activity in the central regions of the remnant. Figure 10 shows a comparison of the star formation rates in fiducial models with and without the finer time steps. For the disk/bulge/halo mergers, the differences are always small, because of the fact that the dense cores do not form until the final stages of the merger and thus do not have time to alter strongly the structure of the inner regions of the remnant. In the disk/halo mergers, the gas clouds form earlier and can subsequently influence the detailed evolution of the centers of the galaxies as they merge. Early in the encounter, differences between the two disk/halo merger simulations are small; only during the final merger is any discrepancy noticeable. The cruder models *underestimate* the amount of dissipation and starburst activity during this phase; however, these differences are minor (a factor of at most a few in starburst intensity) and are apparent for just a brief period, which suggests that qualitative results based on the use of coarse time steps are reliable.

4.2. *A Prograde-Retrograde Merger*

As an example of varying the encounter geometry, we describe in detail the merger of two disk/bulge/halo galaxies from a prograde-retrograde orbit. While many of the

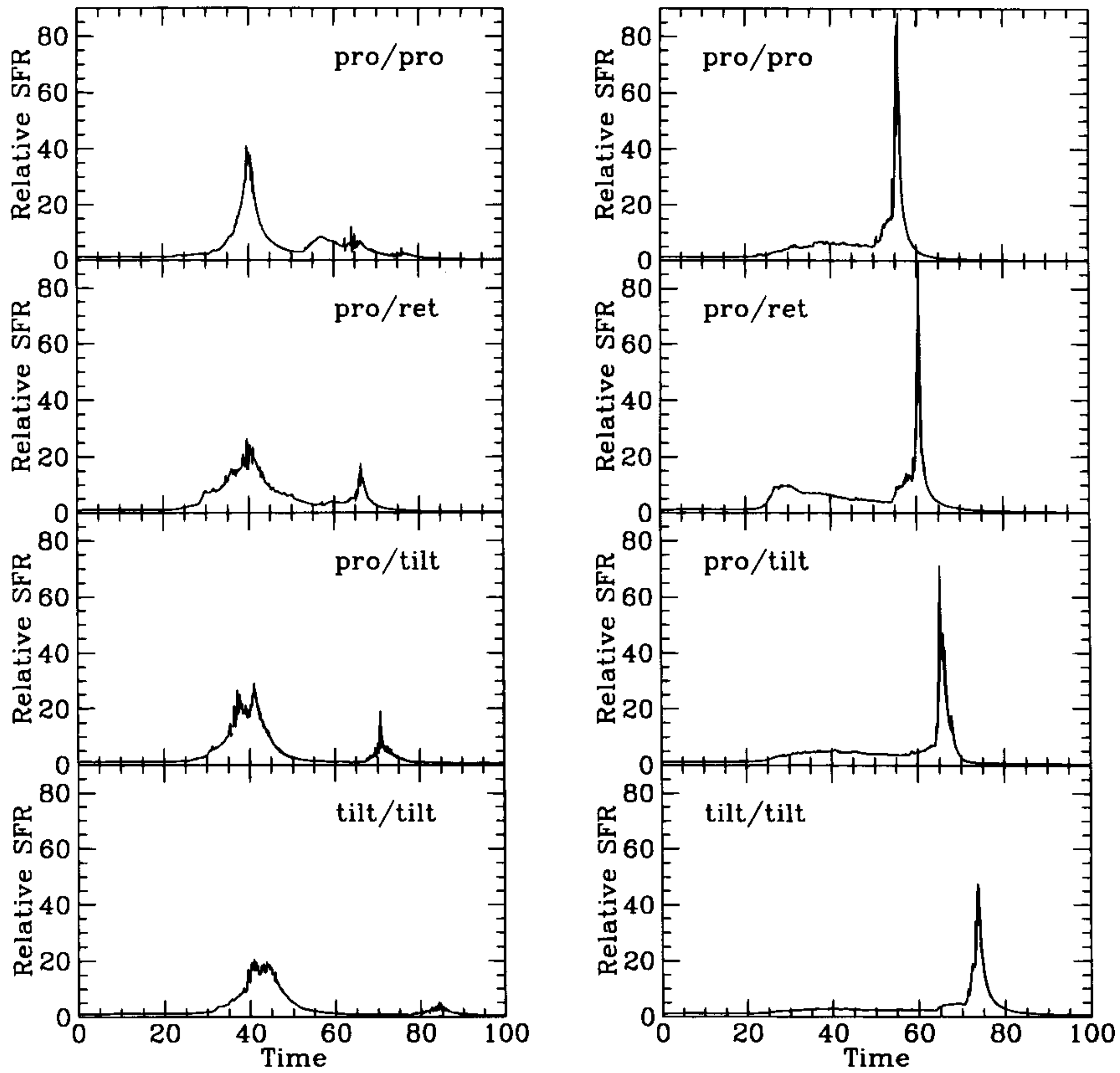

FIG. 14.—Evolution of the global star formation rate for the various model runs. *Left panels*: Disk/halo galaxy mergers. *Right panels*: Disk/bulge/halo galaxy mergers. Star formation rates are measured relative to the total star formation rate in *two* isolated disks.

parameters of this simulation—i.e., the mass ratio, galaxy structure, and orbital type—are identical to the fiducial disk/bulge/halo model shown in Figures 3 and 4, the substitution of a retrograde disk for an inclined disk leads to some interesting differences in the detailed evolution of the merger. First, the retrograde disk experiences a different response since the orbits of particles in the disk are highly nonresonant with the orbital motion of the companion. Second, because of the coplanar nature of this interaction, the potential for strong shocks to develop in the colliding ISMs of the galaxies as they interpenetrate is enhanced.

Figure 11 shows the evolution of the old disk stars during this merger. The prograde disk evolves in largely the same manner as that shown in Figure 3, but the retrograde disk exhibits a markedly different morphology. Because of the lack of a strong resonance between the orbital and rotational motions of the particles in the retrograde disk, tail formation is inhibited. Instead, the disk develops a transient, leading tidal arm in addition to a strong two-armed spiral pattern, as can be seen at, e.g., $t = 28.8$ in Figure 11. Even without the extended tails, the retrograde galaxy still displays distinct morphological features indicative of the collision: tidally induced spiral arms, a central bar, and diffuse tidal debris composed of both its own stars and some stars stripped from the prograde companion. After passing by one another, the galaxies turn around on their orbits and merge, somewhat more rapidly than in the fiducial model of Figure 3. The more rapid merging is likely due to increased drag from the overlapping ISMs of the galaxies; as the galaxies collide, the gas shocks, dissipates energy, and lags the orbital motion of the galaxies, which hastens the braking of the galaxies on their orbits. This effect is enhanced in coplanar mergers, as a larger fraction of the ISM in the galaxies shocks and dissipates energy during the initial impact (see also Mihos 1992; Mihos et al. 1992).

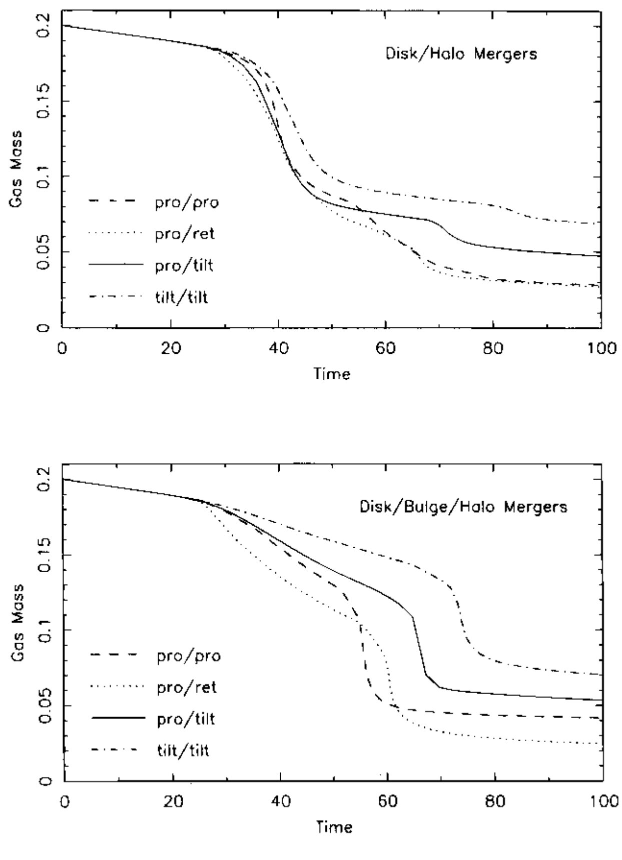

FIG. 15.—Evolution of the total gas mass in the various simulations. *Top*: Disk/halo galaxy mergers. *Bottom*: Disk/bulge/halo galaxy mergers.

The hybrid gas/young star component of the galaxies is shown in Figure 12 and emphasizes even more dramatically the differences from the fiducial encounter. Because the retrograde disk counterrotates with respect to the orbital motion of the companion, gas in the retrograde disk rotates into, rather than away from, the collisional interface of the overlapping ISMs. This situation, coupled with the fact that the collision is coplanar, results in a stronger shock and allows the retrograde disk to sweep up and accrete a substantial fraction ($\sim 30\%$) of the gas in the prograde disk. While the tidal tail of the prograde disk forms mostly out of material traveling on nonintersecting orbits—and is hence gas rich—the spiral features in the stellar component of the retrograde disk are supported by material that has passed through the prograde companion. Because the gas shocks at this interface and cannot freely stream through with the tidal arms, the arms in the retrograde disk are gas poor. Such gas-poor tidal features in an otherwise gas-rich interacting galaxy could therefore serve as a strong indicator of a retrograde collision.

Finally, a map of star formation in the merging pair is shown in Figure 13. As in the fiducial encounter, star formation is boosted in gas initially compressed along the tidal features (see also Mihos & Hernquist 1994b), but most stars formed at intermediate times (i.e., $t = 48$) come from gas that has lost angular momentum and fallen into the inner few kiloparsecs of the galaxies' centers. Interestingly, the star formation rate in the retrograde disk is twice that of the prograde disk at these intermediate times, largely because of the differing gas content of the two galaxies. As noted above, the retrograde disk accretes $\sim 30\%$ of the gas from the prograde disk; furthermore, the prograde disk has temporarily lost another $\sim 15\%$–20% of its gas to its tidal tail. As a result, at this time the retrograde galaxy contains twice the amount of gas as its prograde companion, and this added gas fuels a higher star formation rate (see also Mihos 1994). While the star formation intensity is still rather modest, this finding contrasts with previous suggestions that star formation rates in interacting galaxies will be higher in prograde than retrograde disks. When the galaxies merge at $t \sim 60$, the remaining gas in both disks is rapidly driven to the center of the remnant, which fuels an intense starburst (see § 4.3 below). After the merger is complete, some additional star-forming gas remains in a small central disk.

4.3. *Star-forming Response*

The evolution of the global star formation rate (SFR) for each of the eight mergers is shown in Figure 14. Again, because of the use of a density-dependent Schmidt law to regulate star formation, Figure 14 can be seen equivalently as tracking inflow and gas density. For galaxies with similar structure, the qualitative results are mostly independent of encounter geometry. That is, in the merging disk/halo galaxies, gas inflow occurs shortly after the initial collision, fueling starburst activity while the galaxies are still widely separated. On the other hand, in galaxies that include bulges, the inflow and starburst activity occur late in the merger—regardless of geometry—when the galaxies are coalescing. While geometry certainly plays some role in determining the kinematic and morphological responses of the galaxies, the structure of the galaxies appears to be the decisive factor in terms of the induced starburst activity. Encounter geometry may be more important in distant encounters (see, e.g., Mihos et al. 1992; Mihos 1994) or in mergers of galaxies with bulges significantly less dense than those in our fiducial model (Barnes & Hernquist 1995).

However, while galaxy structure dominates the star-forming response of our models, encounter geometry is not entirely negligible. The most intense inflows and starbursts develop in the coplanar prograde-prograde or prograde-retrograde encounters, while weakest ones occur when the galaxies are both inclined. This effect is most noticeable in plots of the evolving gas content of the various simulations in Figure 15, which measure the time-integrated strength of the induced starbursts. These starbursts deplete $\sim$65% of the gas in the inclined disks, and as much as $\sim$85% of the gas in coplanar mergers. This trend can be explained by more efficient dissipation in the coplanar mergers. Because gas can easily shock and dissipate energy when the disks are coplanar, more of the gas is driven into the central regions in these encounters, which fuels more intense starbursts and results in greater gas depletion. By contrast, in inclined encounters the gas is perturbed onto orbits, which takes it out of the disk plane, reducing the chances of strong dissipation. The gas inflows and associated starbursts are accordingly somewhat weaker than in coplanar mergers.

A second geometrical effect can be seen in the evolution of the merging galaxies: the onset time for the activity is slightly different as the galaxies in the various simulation merge. In the disk/halo models, the strongest inflows occur in the galaxies $\sim$15 time units ($\sim$200 Myr) after the initial collision, regardless of geometry, and can be attributed to the growth of the central bar over a dynamical timescale of the disk. However, in the disk/bulge/halo mergers, the onset of the inflow occurs as early as $t = 55$ for the prograde-prograde galaxy case and as late as $t = 75$ for the merger with both galaxies inclined—a difference of $\sim$250 Myr. Rather than being a consequence of variations in the dissipational history of the gas, this effect simply results from the different coalescence timescales of the mergers. When the galaxies are both prograde, merging occurs rapidly, while mergers of highly inclined galaxies occur more slowly. Therefore, while peak gas densities (and associated starbursts) are achieved at different absolute times (measured from the moment of first collision), they occur at roughly the same dynamical stages of the merging process, when the galaxies are ultimately coalescing and are within a kiloparsec or so of one another.

5. DISCUSSION

5.1. *Theoretical Issues*

5.1.1. *Relation to Previous Results*

The results of this paper reinforce and extend those of earlier studies of gasdynamics in major mergers. In agreement with, e.g., Negroponte & White (1983) and Barnes & Hernquist (1991, 1995), we find that the tidal forces operating on disks during mergers can initiate radial inflows of gas into the nucleus of a remnant, forcing substantial fractions ($\sim$75%) of the gas initially spread throughout both galaxies into localized regions only a few hundred kiloparsecs across. If a density-dependent Schmidt law is appropriate to describe star formation under these extreme conditions, then the densities in these central gas clumps are sufficiently high to trigger short-lived, but powerful, bursts of star formation with rates similar to those observed in the ultraluminous infrared galaxies. This inference generalizes the work of, e.g., Noguchi & Ishibashi (1986) and Mihos et al. (1992, 1993), who discovered that transient encounters between disk galaxies can also induce nuclear starbursts in disks but of considerably weaker intensity than those described in § 3.

5.1.2. *Inflow Mechanism*

By isolating the torques acting on the gas driven to the center of a remnant during a major merger, we have demonstrated that this gas loses angular momentum *gravitationally*, primarily through its interaction with disk stars, substantiating similar claims by, e.g., Noguchi (1987), Combes, Dupraz, & Gerin (1990), and Barnes & Hernquist (1991, 1995). We furthermore show that most of the torque on the gas in a specific disk is contributed by the collisionless matter in the *same* galaxy, rather than by the companion, through the development of large-amplitude, nonaxisymmetric features in the stellar disk. Thus, the gas inflows analyzed here are analogous to those provoked by minor mergers (see, e.g., Hernquist 1989, 1991; Hernquist & Mihos 1995).

However, the basic mechanism responsible for the differences between the response of the gas and the stars in a tidally perturbed disk has yet to be rigorously established. As argued by Barnes & Hernquist (1995), it seems plausible that the dissipational nature of the gas will invariably cause it to lose energy relative to the surrounding collisionless matter when the gravitational potential varies rapidly in time. But in the absence of an underlying theory to describe this aspect of the dynamics, it is less obvious that the gas must also lose angular momentum to the collisionless particles. It is somewhat reassuring, however, that a variety of independent studies have shown that gas inflow appears to occur generically in barred or nonaxisymmetric disks (see, e.g., Schwarz 1984; Athanassoula 1992).

5.1.3. *Influence of Galaxy Structure*

An interesting new finding of the current investigation is the demonstration that the time history of the gas inflows and the resulting starbursts depends sensitively on the detailed structure of the progenitor galaxies. Collisions between disk/halo galaxies lead to prompt inflows shortly after their first close passage, while the gas in similar galaxies having compact bulges suffers this fate only during the *final* stages of a merger. The latter situation appears to be more representative of observed systems which exhibit the most intense starbursts (see, e.g., Sanders 1992).

Superficially, our result appears to be at variance with that of Barnes & Hernquist (1991, 1995) whose mergers of disk/bulge/halo galaxies were accompanied by significant gas inflows immediately after *first* collision. In fact, Barnes & Hernquist employed galaxy models the bulges of which were significantly less concentrated than those described here. We specifically chose parameters so that the rotation curves of our galaxies rise sharply in their inner regions. While we believe that our models are a better description of spirals with relatively massive bulges than those of Barnes & Hernquist, a more systematic survey of the parameter space of galaxy types is clearly needed to compare statistically the simulations to starbursting galaxies.

5.1.4. *Influence of Orbital Geometry*

Perhaps somewhat surprising, the results summarized in § 4 suggest that the onset of activity in galaxy collisions is insensitive to the inclinations of the merging disks. For example, the amount of gas driven to the central regions of the galaxies (and subsequently consumed in the starburst) varies only weakly for varying disk inclinations (see, e.g., Fig. 15). Furthermore, to the extent that our model for star formation is appropriate, the maximum star formation rates in Figure 14 differ by factors of only ~ 2 for the mergers involving the same progenitors but for varying disk inclinations. Unless a more thorough exploration of parameter space predicts different behavior from the cases we considered, it appears unlikely that the relatively modest differences suggested by Figure 14 could be deduced from an observed sample of interacting galaxies, given the more sensitive dependence of starburst intensity to galaxy type. The fact that Keel (1993, 1995) finds that the triggering of starbursts and Seyfert activity in galaxy pairs is more intimately linked to the shape of the galaxies' rotation curves, rather than their inferred orbital geometry, lends observational support to the theoretical results presented here.

As yet, we have not examined the effects of modifying orbit type or impact parameter. The simulations analyzed in §§ 3 and 4 all employed zero-energy orbits with small impact parameters. Barnes & Hernquist (1995) also adopted zero-energy orbits in their modeling but did compare simulations with impact parameters differing from one another by a factor of 2. Although Barnes & Hernquist did not include star formation in their calculations, their results imply that the time history of tidally induced starbursts will depend on impact parameter, as argued by, e.g., Mihos et al. (1992, 1993). Whether or not this effect is as significant as the dependence on galaxy morphology remains to be seen.

5.2. *Relation to Observations*

5.2.1. *Starbursts, Ultraluminous Systems, and AGNs*

Previous theoretical modeling has hinted at the possibility that mergers can explain the ultraluminous infrared galaxies (see, e.g., Barnes & Hernquist 1991). Our work supports these claims by elucidating the mechanisms responsible for triggering gas inflows during galaxy collisions and, furthermore, suggests that star formation rates compatible with those observed are a natural consequence of the dynamics attending these inflows. The results described here, therefore, solidify the apparent observational link between galaxy mergers and the onset of activity in some peculiar galaxies.

Our modeling efforts also shed light on the discrepancy between the merger timescales and the short gas depletion times inferred from observations (see, e.g., Larson 1987; Norman & Scoville 1988; Scoville & Norman 1988; Norman 1988). In particular, previous models of gasdynamics in merging galaxies indicated that inflows of gas occur within a dynamical timescale ($\sim$a few $\times 10^8$ yr) of the initial collision, well before the galaxies ultimately merge (Barnes & Hernquist 1991, 1995; Mihos et al. 1992, 1993). However, observations of ultraluminous systems suggest that the onset of activity occurs largely during the final stages of merging (e.g., Sanders et al. 1988b; Murphy et al. 1995) and that the timescale for starburst activity is very short (10^7–10^8 yr). Our models resolve this discrepancy by showing that the presence of central bulges can delay the onset of activity until the late stages of a merger. Because this result is achieved by inhibiting the dynamical mechanisms which drive inflow, this results is largely independent of the details of assumed Schmidt law for star formation.

The absolute level of starburst activity achieved, however, is more sensitive to our parameterization of the physics of star formation. Within these uncertainties, our models indicate that star formation rates may be elevated by at least 2 orders of magnitude during mergers, as inferred in some observed systems (see, e.g., Solomon, Downes, & Radford 1992). Our findings suggest that an AGN is not required to account for the energy source in these ultraluminous systems. If starbursts alone are responsible for these high luminosities, the implied supernovae rate for a Miller-Scalo (1979) IMF is 1–2 yr^{-1}, which will produce a bright compact radio source in the core of the merger remnant. The radio continuum properties of ultraluminous galaxies may therefore provide a strong observational constraint for this scenario; however, current results are inconclusive (see, e.g., Condon et al. 1991; Lonsdale et al. 1993).

By resolving the timescale discrepancy and achieving ultraluminous levels of starburst activity, our disk/bulge/halo models now provide a good description of the ultraluminous infrared galaxies. Studies of ultraluminous systems show that the highest levels of emission occur preferentially in very close galaxy pairs ($\Delta r \lesssim$ a few kpc) or in single objects, rather than in widely separated galaxy pairs (see, e.g., Sanders et al. 1988b; Murphy et al. 1995). In comparison, when the disk/bulge/halo mergers experience the strongest levels of inflow (and associated starburst activity), they are in the final stages of coalescence, with the galaxies deeply interpenetrating. The morphology of the model galaxies at this point shows distorted, irregular isophotes and extended tidal tails, similar to those seen in optical (see, e.g., Sanders et al. 1988b; Melnick & Mirabel 1990) and 21 cm H I (Hibbard & Yun 1995) studies. Furthermore, the amounts of gas involved in our radial inflows and the sizes of the central gas clumps that develop from them are in reasonable agreement with observations (see, e.g., Scoville et al. 1986; Sargent et al. 1987; Sargent, Sanders, & Phillips 1989; Sanders, Scoville, & Soifer 1991; Tinney et al. 1990; Scoville 1992). Finally, within the uncertainties of the star formation model, the extremely high rates of star formation and the short ($\sim 5 \times 10^7$ yr) duration of the starbursts compare well with the star formation rates and starburst lifetimes inferred for ultraluminous infrared galaxies (see, e.g., Solomon & Sage 1988).

Our simulations are less able to account for the few high-luminosity, large-separation pairs that do exist (Murphy et al. 1995). The disk/bulge/halo models achieve their highest levels of inflow and activity only once they are within a few kiloparsecs of one another, not while they are widely separated. The disk/halo models, on the other hand, are most active during the phase between first collision and the final merging when they are separated by tens of kiloparsecs, but these collisions yield weaker starbursts than their disk/bulge/halo counterparts . However, *gas-rich* disk/halo galaxy mergers could conceivably explain the few widely separated ultraluminous pairs. In fact, it is likely that the progenitor galaxies that develop ultraluminous activity possess a range of structural properties and gas contents and interact under a variety of conditions. Given the strong relationship between structural properties and the timescale and intensity of starbursts in our models, it seems plausible that a properly selected mixture of progenitor galaxies with a range of morphological types could yield a close match to the entire ultraluminous galaxy sample.

It is also interesting that the remnants produced in our simulations exhibit morphological peculiarities similar to many of the brightest radio galaxies (see, e.g., Heckman et al. 1985, 1986; Baum et al. 1988; Baum & Heckman 1989a, b; Smith, Heckman, & Illingworth 1990) and even similar to some low-redshift quasars (see, e.g., Stockton 1978; Heckman et al. 1984; MacKenty & Stockton 1984; Smith et al. 1986; Hutchings 1987; Vader et al. 1987). At present, however, we are unable to clarify the possible connection between galaxy interactions and the origin of AGNs, because of the limited dynamic range of the simulations. Nevertheless, it is plausible that continued fragmentation and collapse of gas in the nuclei of objects like those modeled here will evolve into sources resembling AGNs (see, e.g., Begelman, Blandford, & Rees 1984; Shlosman, Begelman, & Frank 1989).

5.2.2. *Ordinary Galaxies*

With two possible exceptions, discussed below, our calculations support the notion that major mergers of disk galaxies produce objects resembling ellipticals. In particular, loosely bound debris falling into the mostly relaxed remnant produces fine structure like that seen commonly in ordinary ellipticals, such as shells, which were once thought to originate mainly via minor accretion events (see, e.g., Quinn 1984; Hernquist & Quinn 1988, 1989). Similarly, as emphasized by Barnes & Hernquist (1995), warped disks like those discovered in galaxies such as NGC 4753 (Steiman-Cameron, Kormendy, & Durisen 1992) and NGC 5128 (Nicholson, Bland-Hawthorne, & Taylor 1992) are a natural consequence of the late infall of gas into the remnant from material in the tidal tails. Aside from these warped H I disks, such infall can also manifest itself in the form of diffuse "loops" of H I at larger radii, similar to those recently observed in the peculiar ellipticals NGC 5128 and NGC 2865 (Schminovich et al. 1994, 1995).

Star formation has the virtue of depleting the gas so that the amounts of cold gas left in the remnants are in better agreement with normal ellipticals than in the models of, e.g., Barnes & Hernquist (1995). The gas driven to the centers of the remnants is efficiently consumed by the starbursts, leaving behind dense stellar cores and using up most of the gas in each progenitor. However, much of the gas that falls into the remnant at late stages in a merger does not accrete into the center but populates an extended disk, as noted above. In the cases we examined, typically a few $\times\ 10^9\ M_\odot$ worth of cold gas remains, which exhibits no evidence for vigorous star formation. Limits on the total amount of cold gas in ordinary ellipticals are not severe, but our results appear to be in mild conflict with present observational knowledge of normal ellipticals (see, e.g., Bregman, Hogg, & Roberts 1992; see also the recent review by Roberts & Haynes 1994).

Perhaps more worrisome are the stellar residues of the nuclear starbursts. As Mihos & Hernquist (1994c) show, the light profile of the starburst population does not join "seamlessly" onto that of the old stars in the remnant but is instead manifest as a luminosity "spike," in apparent disagreement with the core properties of typical massive ellipticals (see, e.g., Lauer et al. 1995). What is the significance of this result for the merger hypothesis? If it is borne out by further modeling over a wider portion of parameter space and by exploring other descriptions of star formation, it might well rule out the possibility that most ellipticals originate by major mergers of pairs of disk galaxies. Any such claim based on the limited set of calculations done to date is, however, clearly premature, as it is not difficult to imagine mechanisms that could "smooth out" these central spikes. As argued by Barnes & Hernquist (1995), if the stellar cores were subject to a good deal of violent relaxation before finally coalescing into the body of the remnant, their luminosity profiles would presumably be less distinguishable from the old stellar population than in our models. Such an effect might occur for certain parameterizations of star formation, or if remnants like the ones analyzed here were subject to additional merging (for discussions, see, e.g., Hernquist 1993c; Weil & Hernquist 1996).

5.3. *Loose Ends*

5.3.1. *Microphysics*

Given the approximate nature of our description of the ISM, calculations like those discussed here are, at best, caricatures of how the gas in colliding galaxies would actually behave. As emphasized by Barnes & Hernquist (1993), the use of a simple equation of state, whether an isothermal one, as in our simulations, or an ideal gas law combined with nonadiabatic heating and cooling, as employed by Barnes & Hernquist (1995), is not entirely appropriate given that cosmic-ray and magnetic pressure are probably not negligible. A number of authors have argued that these effects, in particular, may enhance the pressures in the centers of galaxies by large factors over that in the local ISM (see, e.g., Spergel & Blitz 1992; Heckman, Armus, & Miley 1990; Suchkov, Allen, & Heckman 1993). Nevertheless, we are encouraged by the similarity of the various calculations to date that have used different equations of state and treatments of radiative effects.

Perhaps more questionable is our neglect of the multiphase structure of the ISM, a limitation necessitated by the relatively poor resolution of the simulations. An SPH description approximates the ISM as a smooth fluid, and, consequently, the gas cannot interpenetrate on small scales as would an ensemble of clouds whose collisional mean free paths are relatively long. If it were averaged over sufficiently large scales, however, it is not implausible that such an ensemble would be well represented by a continuum fluid, and we are again encouraged by the rather good agreement between our results and those which have been obtained using a discrete-cloud model for the ISM (see, e.g., Negroponte & White 1983).

5.3.2. *Star Formation Processes*

Given the lack of resolution on small scales, it is obvious that any treatment of the effects of star formation will be crude and should rightly be viewed with some skepticism. Our parameterization of this process is simple and yields reasonable behavior for the gas in isolated disks over long timescales (Mihos & Hernquist 1994e). However, it is not at all clear that the physical conditions in star-forming regions of quiescent disks are similar to those in the nucleus of a starbursting galaxy. The appropriateness of a Miller-Scalo IMF is somewhat dubious in light of observations suggesting that nuclear starbursts are unusually efficient at producing high-mass stars (see, e.g., Rieke et al. 1980; Doane &

Mathews 1993; Doyon, Joseph, & Wright 1994). Changes in the IMF in our models could significantly alter the amount of gas and energy returned from evolving stars and subsequently impact further star formation. A top-heavy IMF could also modify our prediction for the luminosity profile of the merger core, produce large amounts of hot gas from supernovae, and strongly influence the evolving spectrophotometric properties of the remnant by changing both the metallicity and mass function of the starburst population. Our models should clearly be viewed as being exploratory, insofar as the IMF in starburst galaxies is still poorly constrained.

The best scheme for incorporating feedback into the calculations is also problematic. As discussed in § 2.2, energy is injected to the surrounding gas by newly formed stars in our models through radial impulses delivered to nearby SPH particles. Other workers have experimented with pure thermal input to the gas (see, e.g., Katz 1992; Summers 1993). Based on empirical tests (Mihos & Hernquist 1994e), we believe that our treatment of feedback is well motivated for our application, but simulations of gravitational collapse exhibit sensitivity to the details of the feedback mechanism (see, e.g., Katz & Gunn 1991; Navarro & White 1993). In particular, the rates of inflow and detailed structure of the central starburst population may be modified by employing other schemes for energy release. As such, the lack of a physically self-consistent treatment for handling this feedback is perhaps the weakest aspect of our modeling technique.

5.4. *Future Directions*

Although our calculations have clarified the relevance of gas physics and star formation to the onset of peculiar activity in the nuclei of some galaxies, a number of fundamental questions remain unanswered. Some starburst galaxies are accompanied by outflows ("superwinds") that appear to be linked to the processes responsible for the infrared emission from these systems (see, e.g., Baan, Haschick, & Henkel 1989; Heckman et al. 1990). Thus far, no such winds have developed in any of the relevant numerical simulations and their nature remains a mystery.

The possibility that mergers may trigger the formation of large numbers of star clusters, as may be required to reconcile the merger hypothesis with the specific frequency of globulars around ellipticals versus spirals (see, e.g., Schweizer 1982; Ashman & Zepf 1992; Whitmore et al. 1993), remains unaddressed. Certainly, our models show elevated star formation rates in the collisionally shocked gas, which creates an environment that could be very conducive to forming globular clusters (see, e.g., Murray & Lin 1989, 1992). However, simulations with much larger dynamic range than those presented here will be required to examine this issue in any detail.

We have also called into question the role of major mergers of gas-rich disks to the origin of normal elliptical galaxies. While possibly reconciling the central phase-space densities of spiral progenitors with those of remnant ellipticals, dissipation in the gas may in fact be overly efficient and yield stellar cores that are unlike those of most large ellipticals. Whether or not this result is of basic importance to the origin of early-type galaxies or is instead an artifact of the approximations employed in the simulations is uncertain. If this finding is verified by more refined calculations, it may provide a strong constraint on the fraction of normal ellipticals that formed through mergers of gas-rich disk galaxies.

Finally, the simulations described here explore many different aspects of galaxy evolution, as they follow disk galaxy collisions through the merging process, forming intense starburst activity and leaving behind a remnant that appears strikingly similar to many elliptical galaxies. For the first time, the models tie together in a well-defined manner galaxy mergers, ultraluminous infrared galaxies, and the likely formation history of at least some fraction of the elliptical galaxy population of the local universe. Because of uncertainties in incorporating star formation physics into the models, simulations of the processes discussed here are rightly in their infancy. In the future, refined modeling techniques and higher resolution calculations will make it possible to explore galaxy mergers and starbursts in ever greater detail and place strong constraints on the role played by mergers in driving the evolution of galaxy populations.

We thank Josh Barnes, François Schweizer, and Alar Toomre for helpful discussions. This work was supported in part by the San Diego Supercomputing Center, the Pittsburgh Supercomputing Center, the Alfred P. Sloan Foundation, NASA Theory Grant NAGW-2422, the NSF under grants AST 90-18526 and ASC 93-18185, and the Presidential Faculty Fellows Program. J. C. M. is supported by NASA through a Hubble Fellowship grant HF-01074.01-94A awarded by the Space Telescope Science Institute, which is operated by the Association of Universities for Research in Astronomy, Inc., for NASA under contract NAS 5-26555.

REFERENCES

Armus, L., Heckman, T. M., & Miley, G. 1987, AJ, 94, 831
Armus, L., Surace, J. A., Soifer, B. T., Matthews, K., Graham, J. R., & Larkin, J. E. 1994, AJ, 108, 76
Ashman, K. M., & Zepf, S. E. 1992, ApJ, 384, 50
Athanassoula, E. 1992, MNRAS, 259, 345
Baan, W. A., Haschick, A. D., & Henkel, C. 1989, ApJ, 346, 680
Bahcall, J. N., Kirhakos, S., & Schneider, D. P. 1995a, ApJ, 450, 486
———. 1995b, ApJ, 447, L1
Bahcall, J. N., & Soneira, R. M. 1980, ApJS, 44, 73
Barnes, J. E. 1988, ApJ, 331, 699
———. 1992, ApJ, 393, 484
Barnes, J. E., & Hernquist, L. 1991, ApJ, 370, L65
———. 1992a, AR&A, 40, 705
———. 1992b, Nature, 360, 715
———. 1993, Phys. Today, 46, 3, 54
———. 1995, ApJ, in press
Barnes, J. E., & Hut, P. 1986, Nature, 324, 446
———. 1989a, ApJ, 336, 681
———. 1989b, ApJ, 336, 702
Baum, S. A., Heckman, T., Bridle, L., van Breugel, W., & Miley, G. 1988, ApJS, 68, 643
Begelman, M. C., Blandford, R. D., & Rees, M. J. 1984, Rev. Mod. Phys., 56, 225
Bender, R. 1990a, in Dynamics and Interactions of Galaxies, ed. R. Wielen (Berlin: Springer), 232
———. 1990b, A&A, 229, 441
Bender, R., & Surma, P. 1992, A&A, 258, 250
Berkhuijsen, E. M. 1977, A&A, 57, 9
Bregman, J. N., Hogg, D. E., & Roberts, M. S. 1992, ApJ, 387, 484
Bushouse, H. A. 1986, AJ, 91, 255
———. 1987, ApJ, 320, 49
Caldwell, J. A. R., & Ostriker, J. P. 1981, ApJ, 251, 61
Carlberg, R. G. 1986, ApJ, 310, 593
Combes, F., Dupraz, C., & Gerin, M. 1990, in Dynamics and Interactions of Galaxies, ed. R. Wielen (Berlin: Springer), 205
Condon, J. J., Condon, M. A., Gisler, G., & Puschell, J. J. 1982, ApJ, 252, 102
Condon, J. J., Huang, Z.-P., Yin, Q. F., & Thuan, T. X. 1991, ApJ, 378, 65

Dahari, O. 1984, AJ, 89, 966
Davies, R., et al. 1993, MNRAS, 262, 650
Doane, J. S., & Mathews, W. G. 1993, ApJ, 419, 573
Doyon, R., Joseph, R. D., & Wright, G. S. 1994, ApJ, 421, 101
Duc, P.-A., & Mirabel, I. F. 1994, A&A, 289, 83
Elmegreen, B. G., Kaufman, M., & Thomasson, M. 1993, ApJ, 412, 90
Forbes, D. A., Franx, M., & Illingworth, G. D. 1995, AJ, 109, 1988
Franx, M., & Illingworth, G. D 1988, ApJ, 327, L55
Franx, M., Illingworth, G. D, & Heckman, T. M. 1989, AJ, 98, 538
Gingold, R. A., & Monaghan, J. J. 1977, MNRAS, 181, 375
Goodman, J., & Hernquist, L. 1991, ApJ, 378, 637
Gunn, J. E. 1987, in Nearly Normal Galaxies, ed. S. M. Faber (Berlin: Springer), 455
Heckman, T. M., Armus, L., & Miley, G. K. 1990, ApJS, 74, 833
Heckman, T. M., Bothun, G. D., Balick, B., & Smith, E. P. 1984, AJ, 89, 958
Heckman, T. M., Illingworth, G. D., Miley, G. K., & van Breugel, W. J. M. 1985, ApJ, 299, 41
Heckman, T. M., Smith, E. P., Baum, S. A., van Breugel, W. J. M., Miley, G. K., Illingworth, G. D., Bothun, G. D., & Balick, B. 1986, ApJ, 311, 526
Hernquist, L. 1987, ApJS, 64, 715
———. 1989, Nature, 340, 687
———. 1990a, ApJ, 356, 359
———. 1990b, J. Comp. Phys., 87, 137
———. 1991, Int. J. Supercomput. Appl., 5, 71
———. 1992, ApJ, 400, 460
———. 1993a, ApJ, 409, 548
———. 1993b, ApJS, 86, 389
———. 1993c, in The Environment and Evolution of Galaxies, ed. J. M. Shull & H. A. Thronson, Jr. (Dordrecht: Kluwer), 327
Hernquist, L., & Barnes, J. E. 1991, Nature, 354, 210
———. 1994, in Mass-Transfer Induced Activity in Galaxies, ed. I. Shlosman (Cambridge: Cambridge Univ. Press), 323
Hernquist, L., & Katz, N. 1989, ApJS, 70, 419
Hernquist, L., & Mihos, J. C. 1995, ApJ, 448, 41
Hernquist, L., & Quinn, P. J. 1988, ApJ, 331, 682
———. 1989, ApJ, 342, 1
Hernquist, L., & Spergel, D. N. 1992, ApJ, 399, L117
Hernquist, L., Spergel, D. N., & Heyl, J. S. 1993, ApJ, 416, 415
Hibbard, J., & Mihos, J. C. 1995, AJ, 110, 140
Hibbard, J., & Yun, M. S. 1995, preprint
Hummel, E. 1981, A&A, 96, 111
Hutchings, J. 1987, ApJ, 320, 522
Hutchings, J. B., Crampton, D., & Johnson, A. 1995, AJ, 109, 73
Hutchings, J. B., & Neff, S. G. 1992, AJ, 104, 1
Joseph, R. D. 1990, in Dynamics and Interactions of Galaxies, ed. R. Wielen (Berlin: Springer), 132
Joseph, R. D., Meikle, W. P. S., Robertson, N. A., & Wright, G. S. 1984, MNRAS, 209, 111
Joseph, R. D., & Wright, G. S. 1985, MNRAS, 214, 87
Katz, N. S. 1992, ApJ, 391, 502
Katz, N. S., & Gunn, J. E. 1991, ApJ, 377, 365
Keel, W. C. 1993, AJ, 106, 1771
———. 1995, preprint
Keel, W. C., Kennicutt, R. C., Hummel, E., & van der Hulst, J. M. 1985, AJ, 90, 708
Kennicutt, R. C. 1983, ApJ, 272, 54
———. 1989, ApJ, 344, 685
Kennicutt, R. C., & Keel, W. C. 1984, ApJ, 279, L5
Kennicutt, R. C., Keel, W. C., van der Hulst, J. M., Hummel, E., & Roettiger, K. A. 1987, AJ, 93, 1011
Kleinmann, S. G., et al. 1988, ApJ, 328, 161
Kormendy, J. 1984, ApJ, 287, 577
Kormendy, J., & Sanders, D. B. 1992, ApJ, 390, L53
Larson, R. B. 1987, in Starbursts and Galaxy Evolution, ed. T. X. Thuan, T. Montmerle, & J. T. T. Van (Gif-sur-Yvette: Editions Frontières), 467
Larson, R. B., & Tinsley, B. M. 1978, ApJ, 315, 92
Lauer, T. R., et al. 1995, AJ, submitted
Lawrence, A., Rowan-Robinson, M., Leech, K., Jones, D. H. P., & Wall, J. V. 1989, MNRAS, 240, 329
Leech, K., Penston, M. V., Terlevich, R., Lawrence, A., Rowan-Robinson, M., & Crawford, J. 1989, MNRAS, 240, 349
Lonsdale, C. J., Persson, S. E., & Matthews, K. 1984, ApJ, 287, 95
Lonsdale, C. J., Smith, H. E., & Lonsdale, C. J. 1993, ApJ, 405, L9
Lucy, L. 1977, AJ, 82, 1013
MacKenty, J. W. 1989, ApJ, 343, 125
———. 1990, ApJ, 72, 231
MacKenty, J. W., & Stockton, A. 1984, ApJ, 283, 64
Malin, D. F., & Carter, D. 1980, Nature, 285, 643
McKee, C. F., & Ostriker, J. P. 1977, ApJ, 218, 198
McLeod, K. K., & Rieke, G. H. 1994, ApJ, 431, 137
Melnick, J., & Mirabel, I. F. 1990, A&A, 231, L19
Mihos, J. C. 1992, Ph.D. thesis, Univ. of Michigan
———. 1994, in Mass Transfer Induced Activity in Galaxies, ed. I. Shlosman (Cambridge: Cambridge Univ. Press), 372
Mihos, J. C., Bothun, G. D., & Richstone, D. O. 1993, ApJ, 418, 82
Mihos, J. C., & Hernquist, L. 1994a, ApJ, 425, L13
———. 1994b, ApJ, 431, L9
———. 1994c, ApJ, 437, L47
Mihos, J. C., & Hernquist, L. 1994d, ApJ, 427, 112
———. 1994e, ApJ, 437, 611
Mihos, J. C., Richstone, D. O., & Bothun, G. D. 1992, ApJ, 400, 153
Miller, G. E., & Scalo, J. M. 1979, ApJS, 41, 513
Mirabel, I. F., Dottori, H., & Lutz, D. 1992, A&A, 256, L19
Mirabel, I. F., Lutz, D., & Maza, J. 1991, A&A, 243, 367
Mongahan, J. J. 1992, AR&A, 30, 543
Mongahan, J. J., & Gingold, R. A. 1983, J. Comp. Phys., 52, 374
Mongahan, J. J., & Lattanzio, J. C. 1985, A&A, 149, 135
Murphy, T. W., et al. 1995, preprint
Murray, S. D., & Lin, D. N. C. 1989, ApJ, 339, 933
———. 1992, ApJ, 400, 265
Navarro, J. F., & White, S. D. M. 1993, MNRAS, 265, 271
Negroponte, J., & White, S. D. M. 1983, MNRAS, 205, 1009
Nicholson, R. A., Bland-Hawthorn, J., & Taylor, K. 1992, ApJ, 387, 503
Noguchi, M. 1987, MNRAS, 228, 635
———. 1988, A&A, 203, 259
———. 1991, MNRAS, 251, 360
Noguchi, M., & Ishibashi, S. 1986, MNRAS, 219, 305
Norman, C. 1988, in Galactic and Extragalactic Star Formation, ed. R. E. Pudritz & M. Fich (Dordrecht: Reidel), 495
Norman, C., & Scoville, N. 1988, ApJ, 332, 124
Olson, K. M., & Kwan, J. 1990a, ApJ, 349, 480
———. 1990b, ApJ, 361, 426
Osterbrock, D. E. 1993, ApJ, 404, 551
Peletier, R. F., Davies, R. L., Illingworth, G. D., Davis, L. E., & Cawson, M. 1990, AJ, 100, 1091
Press, W. H., Flannery, B. P., Teukolsky, S. A., & Vetterling, W. T. 1986, Numerical Recipes: The Art of Scientific Computing (Cambridge: Cambridge Univ. Press)
Rieke, G. H., Lebofsky, M. J., Thompon, R. I., Low, F. J., & Tokunaga, A. T. 1980, ApJ, 238, 24
Roberts, M. S., & Haynes, M. P. 1994, AR&A, 32, 115
Quinn, P. J. 1984, ApJ, 279, 596
Sanders, D. B. 1992, in ASP Conf. Proc. 31, Relationships between Active Galactic Nuclei and Starburst Galaxies, ed. A. V. Fillipenko (San Francisco: ASP), 303
Sanders, D. B., Scoville, N. Z., Sargent, A. I., & Soifer, B. T. 1988a, ApJ, 324, L55
Sanders, D. B., Scoville, N. Z., & Soifer, B. T. 1991, ApJ, 370, 158
Sanders, D. B., Soifer, B. T., Elias, J. H., Madore, B. F., Matthews, K., Neugebauer, G., & Scoville, N. Z. 1988b, ApJ, 325, 74
Sanders, D. B., Soifer, B. T., & Neugebauer, G. 1990, in Dynamics and Interactions of Galaxies, ed. R. Wielen (Berlin: Springer), 459
Sanders, D. B., Young, J. S., Scoville, N. Z., Soifer, B. T., & Danielson, G. E. 1987, ApJ, 312, L5
Sanders, D. B., et al. 1986, ApJ, 305, L45
Sargent, A. I., Sanders, D. B., & Phillips, T. G. 1989, ApJ, 346, L9
Sargent, A. I., Sanders, D. B., Scoville, N. Z., & Soifer, B. T. 1987, ApJ, 312, L35
Sargent, A., & Scoville, N. Z. 1991, ApJ, 366, L1
Schiminovich, D., van Gorkom, J. H., van der Hulst, J. M., & Kasow, S. 1994, ApJ, 423, L101
Schiminovich, D., van Gorkom, J. H., van der Hulst, J. M., & Malin, D. 1995, ApJ, 444, L77
Schmidt, M. 1959, ApJ, 129, 243
Schwarz, M. P. 1984, MNRAS, 209, 93
Schweizer, F. 1978, in Structure and Properties of Nearby Galaxies, ed. E. M. Berkhuijsen & R. Wielebinski (Dordrecht: Reidel), 279
———. 1982, ApJ, 252, 455
———. 1990, in Dynamics and Interactions of Galaxies, ed. R. Wielen (Berlin: Springer), 60
Schweizer, F., & Seitzer, P. 1988, ApJ, 328, 88
Scoville, N. Z. 1992, in ASP Conf. Proc. 31, Relationships between Active Galactic Nuclei and Starburst Galaxies, ed. A. V. Filipenko (San Francisco: ASP), 159
Scoville, N., & Norman, C. 1988, ApJ, 332, 163
Scoville, N. Z. Sanders, D. B., Sargent, A. I., Soifer, B. T., Scott, S. L., & Lo, K. Y. 1986, ApJ, 311, L42
Scoville, N. Z., Sargent, A. I., Sanders, D. B., & Soifer, B. T. 1991, ApJ, 366, L5
Shlosman, I., Begelman, M. C., & Frank, J. 1990, Nature 345, 679
Smith, E., & Heckman, T. M. 1989a, ApJS, 69, 365
———. 1989b, ApJ, 341, 658
Smith, E., Heckman, T. M., Bothun, G., Romanshin, W., & Balick, B. 1986, ApJ, 306, 64
Smith, E., Heckman, T. M., & Illingworth, G. D. 1990, ApJ, 356, 399
Soifer, B. T., et. al. 1984a, ApJ, 278, L71
Soifer, B. T., et. al. 1984b, ApJ, 283, L1
Solomon, P. M., Downes, D., & Radford, S. J. E. 1992, ApJ, 387, L55
Solomon, P. M., & Sage, L. J. 1988, ApJ, 334, 613
Spergel, D. N., & Blitz, L. 1992, Nature, 357, 665
Stanford, S. A., & Bushouse, H. A. 1991, ApJ, 371, 92
Steiman-Cameron, T. Y., Kormendy, J., & Durisen, R. H. 1992, AJ, 104, 1339
Stockton, A. 1978, ApJ, 223, 747
———. 1990 in Dynamics and Interactions of Galaxies, ed. R. Wielen (Berlin: Springer), 440

Suchkov, A., Allen, R. J., & Heckman, T. M. 1993, ApJ, 413, 542
Summers, F. 1993, Ph.D. thesis, Univ. of California, Berkeley
Surma, P., & Bender, R. 1995, A&A, 298, 405S
Tinney, C. G., Scoville, N. Z., Sanders, D. B., & Soifer, B. T. 1990, ApJ, 362, 471
Toomre, A. 1962, ApJ, 138, 385
———. 1977 in The Evolution of Galaxies and Stellar Populations, ed. B. Tinsley & R. Larson (New Haven: Yale Univ. Press), 401
———. 1981, in The Structure and Evolution of Normal Galaxies, ed. S. M. Fall & D. Lynden-Bell (Cambridge: Cambridge Univ. Press), 111
Toomre, A., & Toomre, J. 1972, ApJ, 178, 623
Vader, J. P., Da Costa, G. S., Frogel, J. A., Heisler, C. A., & Simon, M. 1987, AJ, 94, 847
van Albada, T. S., Kotanyi, C. G., & Schwarzschild, M. 1982, MNRAS, 198, 303
van Gorkom, J. H., van der Hulst, J. M., Haschick, A. D., & Tubbs, A. D. 1990, AJ, 99, 1781
Veilleux, S., Kim, D.-C., Sanders, D. B., Mazzarella, J. M., & Soifer, B. T. 1995, ApJS, 98, 171
Weil, M. L., & Hernquist, L. 1996, ApJ, 460, 101
Wright, G. S., James, P. A., Joseph, R. D., & McLean, I. S. 1990, Nature, 344, 417
Whitmore, B. C., Schweizer, F., Leitherer, C., Borne, K., & Robert, C. 1993, AJ, 106, 1354
Zwicky, F. 1956, Egreb. Exakt. Naturwiss., 29, 344